

1 **From thirteen to twenty-two in a second stroke: revisiting the European *Eumida sanguinea***  
2 **(Phyllodoceidae: Annelida) species complex**

3  
4 Marcos A.L. Teixeira<sup>1,2\*</sup>, Pedro E. Vieira<sup>1,2</sup>, Ascensão Ravara<sup>4</sup>, Filipe O. Costa<sup>1,2</sup>, Arne Nygren<sup>3</sup>

5 <sup>1</sup> Centre of Molecular and Environmental Biology (CBMA), Department of Biology, University of  
6 Minho, Campus de Gualtar, 4710-057, Braga, Portugal

7 <sup>2</sup> Institute of Science and Innovation for Bio-Sustainability (IB-S), University of Minho, Campus de  
8 Gualtar, 4710-057, Braga, Portugal

9 <sup>3</sup> Institutionen for marina vetenskaper, Göteborgs Universitet, Tjärnö, Strömstad, Sweden

10 <sup>4</sup> Centre for Environmental and Marine Studies (CESAM), Department of Biology, University of  
11 Aveiro, Campus de Santiago, 3810-193 Aveiro, Portugal.

12  
13 *\*Corresponding author*

14 Mail: mark-us\_teixeira@hotmail.com

15  
16 **Running Title:** Revisiting the *Eumida sanguinea* species complex

17  
18  
19  
20 **FUNDING AND ACKNOWLEDGMENTS**

21 This study was supported by the project NextSea (NORTE-01-0145-FEDER-000032),  
22 under the PORTUGAL 2020 Partnership Agreement, through the European Regional  
23 Development Fund (ERDF). Thanks are due, for the financial support to CESAM  
24 (UIDB/50017/2020+UIDP/50017/2020), to FCT/MEC through national funds, and the co-funding  
25 by the FEDER, within the PT2020 Partnership Agreement and Compete 2020. Marcos A.L.  
26 Teixeira was supported by a PhD grant from FCT co-financed by ESF (SFRH/BD/131527/2017).  
27 Pedro Vieira work was supported by national funds through the Portuguese Foundation for  
28 Science and Technology (FCT, I.P.) in the scope of the project NIS-DNA [PTDC/BIA-  
29 BMA/29754/2017]. Ascensão Ravara was funded by national funds (OE), through FCT, I.P., in  
30 the scope of the framework contract foreseen in the numbers 4, 5 and 6 of the article 23, of the  
31 Decree-Law 57/2016, of August 29, changed by Law 57/2017, of July 19. Financial support to  
32 Arne Nygren from the Norwegian Taxonomy Initiative [<http://www.biodiversity.no/Pages/135523>]  
33 (Cryptic polychaete species in Norwegian waters, knr 49-13, pnr 70184228), the Swedish  
34 Taxonomy Initiative [<https://www.artdatabanken.se/en/the-swedish-taxonomy-initiative/>]  
35 (Polychaete species complexes in Swedish waters, dnr 140/07 1.4 and 166/08 1.4), and Kungliga  
36 Fysiografiska sällskapet Nilsson-Ehle donationerna [<https://www.fysiografen.se/sv/>].

40  
41  
42  
43  
44  
45  
46  
47  
48  
49  
50  
51  
52  
53  
54  
55  
56  
57  
58  
59  
60  
61  
62  
63  
64  
65  
66  
67  
68  
69  
70  
71  
72  
73  
74  
75  
76  
77  
78  
79

**ABSTRACT**

*Eumida sanguinea* is a recognized polychaete species complex which, in previous studies, has been reported to have additional undescribed diversity. We detected nine additional lineages by analysing DNA sequence (mitochondrial: COI, 16S rRNA and nuclear loci: ITS region and 28S rRNA) of *E. sanguinea* morphotype populations from a broader sampling effort in European marine waters. Customary morphological features failed to provide consistent differences or unique characters that could be used to distinguish these *Eumida* species. However, by complementing DNA data with morphometrics, geographic range, colour, and pigmentation patterns, we revealed five new species. Two of these undescribed species derived from the previously signalled *Eumida* lineages S21 and GB22, which are now named as *E. schanderi* sp. nov. and *E. fenwicki* sp. nov., respectively. Three other species based on newly discovered lineages, namely *E. gretathunbergae* sp. nov., *E. pleijeli* sp. nov., and *E. langenecki* sp. nov. From the six new lineages remaining, three are represented by less than two exceptionally well-preserved specimens, which prevented further comprehensive analysis. The last three lineages were only distinct with mitochondrial markers. Integrative taxonomy is essential to elucidate evolutionary phenomena and eventually allow informed use of species complexes, exhibiting stasis in biomonitoring or other ecological studies.

**ADDITIONAL KEYWORDS:** *Eumida*, Phyllodocidae, pigmentation, morphological stasis

80

81

## 82 INTRODUCTION

83         The species *Eumida sanguinea* (Örsted, 1843) was originally described from the Danish  
84 coast (WoRMS Editorial Board, 2021) and has been commonly reported in the Atlantic northern  
85 hemisphere (Eibye-Jacobsen, 1991), including the northern Iberian Peninsula (Leite *et al.*, 2019),  
86 as well as in Madagascar, Mozambique (Day *et al.*, 1967), and New Zealand (Glasby *et al.*, 2009).  
87 It is usually found in sandy-muddy substrates or gravel and among algae in shallow subtidal  
88 habitats, ranging from a few to hundreds of meters in depth (Eibye-Jacobsen, 1991), including  
89 estuaries and coastal lagoons (Walker & Rees, 1980). As a phyllodocid, it is believed to be a  
90 carnivore (Jumars, Dorgan, & Lindsay, 2015), but no published study has yet described its specific  
91 feeding habits. Although its planktotrophic larvae enable a large-scale dispersal (Pleijel, 1993;  
92 Rouse, 2006) its cosmopolitan status has recently been challenged. In European seas, 13  
93 different lineages have already been reported to belong to the *Eumida sanguinea* species  
94 complex (*Essc*). By combining multi-locus molecular data with the white pigmentation pattern  
95 observed in live animals, Nygren & Pleijel (2011) defined nine of those lineages as nominal  
96 species: *Eumida sanguinea* s.s.; *Eumida notata* (Langerhans, 1880); *Eumida alkyone* Nygren &  
97 Pleijel, 2011; *E. asterope* Nygren & Pleijel, 2011; *E. elektra* Nygren & Pleijel, 2011; *E. kelaino*  
98 Nygren & Pleijel, 2011; *E. maia* Nygren & Pleijel, 2011; *E. merope* Nygren & Pleijel, 2011; and *E.*  
99 *taygete* Nygren & Pleijel, 2011. More recently, Teixeira *et al.* (2020) delineated another species  
100 from the complex, *Eumida mackiei* Teixeira, Pleijel & Nygren, by adding quantitative  
101 morphometric analyses to the methodology used in the previous study. The remaining putative  
102 species [*Eumida* F22 and *Eumida* S21 from Nygren & Pleijel (2011)], and *Eumida* GB22 from  
103 Teixeira *et al.* (2020), could not be described because only one specimen of each was available,  
104 which is not ideal, especially when the description is heavily based on molecular data (Churchill  
105 *et al.*, 2014; Delić *et al.*, 2017) and morphometric analyses (Ravara, *et al.*, 2010; Martin *et al.*,  
106 2017). All these putative species appeared to be sympatric with at least one other species of the  
107 complex, except for *E. notata* that is exclusive to Madeira Island (Portugal) and possesses a  
108 unique white pigmentation pattern among the *Essc*. However, there was no consensus between  
109 mitochondrial and nuclear loci sequences (Teixeira *et al.*, 2020) in the segregation of *E. notata*  
110 from its sister Mediterranean species, *Eumida merope*, as separate molecular operational  
111 taxonomic units (MOTUs).

112         The new *Essc* illustrated in Nygren & Pleijel (2011) were described based on systematic  
113 molecular analyses, an approach applicable when there are no evident morphological differences  
114 (cryptic species). Apart from the white pigmentation pattern in live worms, the morphology of  
115 antennae, anterior cirri, and parapodia provided no consistent differences to be used to  
116 distinguish species. Moreover, all setae are composite within the entire genus (Pleijel, 1993). As  
117 seen in Teixeira *et al.* (2020), slight differences in shape and length of dorsal and ventral cirri, in  
118 the anterior appendages, or distance between eyes and head width can be further explored by  
119 morphometric analyses. However, intraspecific and size-dependent variations are large and can

120 fail to produce independent clusters. The presence and arrangement of proboscis papillae may  
121 be distinctive traits; however, the proboscis is often not everted, and papillae are sometimes  
122 difficult to detect in preserved specimens. Nevertheless, Teixeira *et al.* (2020) reported the  
123 presence of proboscis papillae in *E. maia* as opposed to the smooth appearance described for *E.*  
124 *sanguinea* s.s. (Pleijel, 1993). Reproductive features and gametogenesis may be a useful  
125 alternative in discriminating closely related species, as seen in Sampieri *et al.* (2020), in which  
126 two cryptic *Laeonereis* (family Nereididae) lineages were distinguished using both COI and  
127 histological data. However, specimens have to be directly preserved in a special preservation  
128 solution (e.g., 10% glutaraldehyde) instead of ethanol, which, in turn, may affect DNA  
129 amplification success.

130 Morphological stasis has been pointed to as a possible justification for morphological  
131 similarities within cryptic complexes, wherein some members retain a high degree of  
132 morphological similarity over extended periods (Costa & Carvalho, 2010; Cerca *et al.*, 2020b).  
133 Although it has been investigated by combining comprehensive data on genomic and phenotypic  
134 traits to statistically test for significant differences in rates of phenotypic disparity between cryptic  
135 and non-cryptic species (Struck *et al.*, 2018), stasis remains a controversial issue in evolutionary  
136 biology (Crossman *et al.*, 2016; Fraïsse *et al.*, 2016; Fišer *et al.* 2018). Morphological characters  
137 and their variation are important to identify and discriminate specimens and species; therefore,  
138 their absence is often interpreted as a potential failure to capture and study biodiversity (Futuyma,  
139 2010). Finding new cryptic lineages and combining molecular tools with occasional small  
140 morphological trait changes in lineages displaying stasis is essential to help comprehend this  
141 evolutionary phenomenon.

142 In this study, nine new *Essc* lineages were uncovered in the European NE Atlantic and  
143 Mediterranean Sea, with five of them being erected to accommodate the previously undescribed  
144 *Eumida* S21 (Nygren & Pleijel, 2011) and *Eumida* GB22 (Teixeira *et al.*, 2020), and three of them  
145 unravelled for the first time. The lineages were defined based on four different loci and  
146 supplemented by data on morphometrics, geographic range, colour, and pigmentation patterns.  
147 Furthermore, new sequences were provided for the previously described species, both from  
148 populations already located such as *E. maia* from Great Britain (Plymouth), *E. taygete* from  
149 France (Banyuls), and *E. alkyone* from Norway (Bergen and Drøbak), as well as unreported  
150 locations like *E. kelaino* from Great Britain (Plymouth), France (Roscoff), and Norway (Sandefjord  
151 and Bergen); *E. merope* from Great Britain (Plymouth) and France (Roscoff); *E. elektra* from  
152 France (Roscoff); *E. sanguinea* s.s. from Great Britain (Plymouth); and lastly *E. taygete* from  
153 Great Britain (Plymouth) and western Italy (Ischia). The close molecular similarity between some  
154 of the new lineages was discussed from an evolutionary perspective, and the *Essc* case was used  
155 to investigate links between morphological stasis and cryptic diversity.

156

## 157 MATERIAL AND METHODS

158

### 159 TAXON SAMPLING, IMAGE CAPTURE, AND MOLECULAR DATA RETRIEVAL

160 One hundred and forty-eight *Eumida* specimens were collected from Norway (Agdenes –  
161 NOA; Bergen – NOB; Drøbak – NOD; and Sandefjord - NOS), Sweden (Bohuslän - SWB), France  
162 (Roscoff - FRR and Banyuls - FRB), Great Britain (Plymouth – GBP and Cornwall - GBC), and  
163 Italy (Ischia – ITI; Taranto – ITT; Antignano – ITA; Naples – ITN; and Orbetello - ITO) and fixed  
164 in 96% ethyl alcohol for molecular analysis. Photographs of live and preserved specimens were  
165 taken with a Canon EOS1100D camera. The specimens from Norway are deposited at the  
166 University Museum of Bergen (ZMBN), and the remaining ones at the Biological Research  
167 Collection (Marine Invertebrates) of the Department of Biology of the University of Aveiro (COBI  
168 at DBUA), Portugal. Additional specimens of *E. merope* and *E. notata* were kindly loaned by the  
169 Swedish Museum of Natural History (SMNH), and COBI-DBUA. The two specimens of *E. taygete*,  
170 MTANE128-19 and MTANE129-19, had all their tissue used for DNA extraction purposes, and no  
171 voucher is available.

172 We obtained sequences of mitochondrial cytochrome oxidase subunit I (mtCOI-5P) from  
173 all the new available 148 specimens, and mitochondrial 16S rRNA, nuclear ITS-regions (i.e., ITS1,  
174 5.8S rRNA, and ITS2), and 28S rRNA for a representative number of specimens per location. For  
175 comparison purposes, a compilation of 149 published sequences from the mtCOI, as well as 100  
176 sequences from the ITS-regions and 28S rRNA corresponding to the *Essc*, and the respective  
177 outgroups were mined from the GenBank, originally from the studies of Nygren & Pleijel (2011)  
178 and Teixeira *et al.* (2020). Moreover, 35 novel 16S sequences were retrieved during this work  
179 from specimens used in the previous studies. Molecular data from *Eumida bahusiensis*  
180 Bergström, 1914; *Eumida ockelmanni* Eibye-Jacobsen, 1987; and *Sige fusigera* Malmgren, 1865  
181 were used as outgroups for all alignments to comprise the final dataset. The full dataset and  
182 associated metadata can be accessed at the Barcode of Life Data Systems (BOLD), under the  
183 project “Five new species - *Eumida sanguinea* complex (DS-MTANE2)” and in the following link:  
184 DOI: [dx.doi.org/10.5883/DS-MTANE2](https://doi.org/10.5883/DS-MTANE2). Table S1 details the sampling locations, GenBank  
185 accession numbers, and voucher data. DNA was extracted, amplified, sequenced, and  
186 assembled as described in Nygren *et al.* (2018). Table 1 displays the PCR conditions and primers  
187 used.

188

## 189 PHYLOGENETIC ANALYSIS AND GENETIC DISTANCES

190 A methodology similar to that of Teixeira *et al.* (2020) was applied for the phylogenetic  
191 analysis of the different loci by maximum likelihood (ML) and Bayesian inference (BI). In brief,  
192 mitochondrial markers (COI and 16S) were concatenated and aligned in MEGA 10.0.5 software  
193 (Kumar *et al.*, 2018) with Clustal W (Thompson *et al.*, 1994). Nuclear markers (ITS regions and  
194 28S) were also concatenated and aligned with MAFFT online ([https://  
195 mafft.cbrc.jp/alignment/server/](https://mafft.cbrc.jp/alignment/server/); Katoh & Standley, 2013). Table 1 included all marker sequence  
196 lengths. Highly variable regions, extensive gaps, and poorly aligned positions, which were  
197 extensively present only in the concatenated nuclear alignment, were eliminated using Gblocks  
198 0.91b ([http://molevol.cmima.csic.es/castresana/Gblocks\\_server.html](http://molevol.cmima.csic.es/castresana/Gblocks_server.html); Castresana, 2000). The  
199 options for a less stringent selection and to not allow many contiguous non-conserved positions

200 were selected, making it more suitable for phylogenetic analysis. We used MrBayes 3.1.2  
201 (Ronquist & Huelsenbeck, 2003) to conduct the Bayesian analysis. Best-fit models were selected  
202 using the Akaike Information Criterion in the JModeltest software (Guindon & Gascuel, 2003;  
203 Darriba *et al.*, 2012). For COI, we applied the Hasegawa-Kishino-Yano with gamma-distributed  
204 rates across sites (HKY +G) for the third position and the General Time-Reversible (GTR) model  
205 with equal rates across sites (GTR) for the first two positions. The latter was also applied to the  
206 16S analysis. Regarding the concatenated ITS region with 28S, we applied the GTR model with  
207 gamma-distributed rates across sites (GTR +G). The number of generations was set to 10 000  
208 000, and the sampling frequency to 500. Twenty-five per cent of the samples were discarded as  
209 burn-in (burninfrac = 0.25). The resulting tree files were successfully checked for convergence in  
210 Tracer 1.6 software (Rambaut *et al.*, 2018) and then analysed in Figtree 1.4.3  
211 (<http://tree.bio.ed.ac.uk/software/figtree/>). The final version of the trees for each alignment was  
212 edited with the software Inkscape 0.92.3 (<https://www.inkscape.org>). Maximum likelihood  
213 phylogenies were performed in MEGA 10.0.5 with 1 000 bootstrap runs, using the GTR model  
214 with equal rates across sites for both concatenated datasets. Only the BI tree was displayed in  
215 the results and, in the case of a similar topology, with the addition of the ML support values. The  
216 alignments (FASTA and NEXUS formats) for each marker and the concatenated ones are all  
217 publicly available online at Figshare (DOI: 10.6084/m9.figshare.12114528 ).

218 The mean genetic distances (Kimura-2-parameters, K2P) within and between MOTUs  
219 were calculated in MEGA 10.0.5, using the same GBlock alignment from above for nuclear loci.

220

## 221 MOTU CLUSTERING

222 To depict MOTUs, we applied three delineation methods to both the concatenated  
223 mitochondrial and nuclear alignments except for COI, to which we also applied the Barcode Index  
224 Number (BIN), implemented in BOLD (Ratnasingham & Hebert, 2013), which is exclusive to this  
225 locus. The Automatic Barcode Gap Discovery (ABGD, Puillandre *et al.*, 2012) approach was  
226 implemented on a web interface (<http://www.wabi.snv.jussieu.fr/public/abgd/abgdweb.html>) with  
227 default settings and K2P distance matrix. Both Generalized Mixed Yule Coalescent (GYMC)  
228 single threshold model (Fujisawa & Barraclough, 2013) and Poisson Tree Processes (bPTP,  
229 Zhang *et al.*, 2013) were applied on a web interface (<https://species.h-its.org/>). BEAST 2.4.6  
230 (Bouckaert *et al.*, 2014) was used to generate a Bayesian ultrametric tree for the GYMC, with the  
231 appropriate best model (based on AIC criteria; GTR equal rates) and four independent runs for  
232 50 000 000 MCMC generations, sampled every 5 000 generations. Tracer 1.6 software was used  
233 to estimate convergence in effective sampling sizes (ESSs > 200) for all parameters. A consensus  
234 tree was obtained using TreeAnnotator 2.4.6 (Bouckaert *et al.*, 2014) and loaded into the Figtree  
235 software. The ML phylogenies obtained in the “phylogenetic analysis” section contributed to the  
236 bPTP results. Consensus MOTUs were defined based on the majority rule and, in case of a draw,  
237 an intermediate MOTU was chosen.

238

## 239 GENETIC DIVERSITY AND STRUCTURE

240 To evaluate the relationship between haplotypes and their geographical distribution,  
241 haplotype networks were built through the PopART software (Leigh & Bryant, 2015) using the  
242 TCS method (Clement *et al.*, 2002). No GBlocks were applied in this analysis to avoid  
243 underestimating the number of nuclear haplotypes. Indices of genetic diversity, namely number  
244 of haplotypes (h), haplotype diversity (HD), polymorphic sites (S), nucleotide diversity ( $\pi$ ), and Fu  
245 & Li D and Tajima D statistical tests, were estimated based on COI for each MOTU, using the  
246 DNASP 5.10 software (Librado & Rozas, 2009).

247

#### 248 MORPHOMETRY

249 Two objectives were proposed for morphometric analysis, namely: (1) to explore if  
250 genetically similar species belonging to *E. notata*, *E. merope*, and the new British lineage *E. aff.*  
251 *merope* can be separated using the methodology and (2) to complement molecular results with  
252 morphometric data to help describe the new species *E. schanderi* sp. nov., *E. fenwicki* sp. nov.,  
253 and *E. gretathunbergae* sp. nov. Since in the previous study (Teixeira *et al.*, 2020), *E. sanguinea*  
254 s.s. showed high morphometric intraspecific variability and failed to produce an independent  
255 morphometric cluster, we used new samples of *E. elektra* for comparison purposes. This species  
256 was chosen for being usually located in the middle of the phylogenetic tree and within the average  
257 *Essc* genetic distances.

258 The remaining lineages were represented by very small and/or less than three specimens  
259 and thus were not used for this analysis. At least nine preserved specimens under ideal conditions  
260 (i.e., with the morphological characters proposed herein and, if possible, of similar sizes) were  
261 chosen per population. All the different morphological characters were measured directly from the  
262 specimen, without dissecting specific structures.

263 The following characters were selected and measured (Fig. 1A-B): number of segments  
264 (NS); the lengths (in mm) of worm (WL), chaetigerous lobes (CLL), terminal antennae (AL), palps  
265 (PL), median antenna (MAL), cirri on segment 1 and dorsal cirri on segment 2 (CS1L, DCS2L),  
266 dorsal and ventral cirri on median segments (DCL, VCL), and head (HL); the widths (in mm) of  
267 worm with parapodia (WWP) and without parapodia (WW), head (HW), and dorsal and ventral  
268 cirri of median segments (DCW, VCW); and distance between eyes (DE), as well as height (mm)  
269 of chaetigerous lobes (CLH). Although the first two segments are fused, we refer to them as  
270 segments 1 and 2, with the latter having a pair of cirri (dorsal and ventral). WW and WWP were  
271 measured from the worm's widest part, usually from either segment 27 or 40, depending on the  
272 worm's size. The distance between eyes was measured from the centre of the eyespots to avoid  
273 possible different individual responses to fixation as is the case of hesionids (Martin *et al.*, 2017).  
274 To minimize bias based on size variability, measurements taken for inter-population analysis were  
275 converted to ratios and used to create scatter plots for the following pairs of morphological  
276 characters: AL/STL, AL/LTL, AL/HL, AL/HW, AL/PL, AL/MAL, PL/MAL, HL/MAL, HW/MAL,  
277 STL/LTL, LTL/HL, STL/HL, PL/STL, PL/LTL, DE/HL, DE/WW, HL/HW, WW/WWP, WW/NS,  
278 WL/NS, WW/WL, HL/MAL, DCL/VCL, DCL/DCW, VCL/VCW, DCL/CLL, VCL/CLL, and CLL/CLH.  
279 The scatter plots were produced using Microsoft Excel (Office 365 ProPlus).

280 Although not used in the above analysis due to lack of available specimens in optimal  
281 conditions to allow the creation of morphometric clusters, additional measurements were also  
282 collected for two Italian lineages (*E. pleijeli* sp. nov. and *E. langenecki* sp. nov.). The ratio of  
283 common morphological structures used to separate *Eumida* species might provide additional  
284 information to be used as differential diagnoses against the remaining analysed lineages.  
285 Emphasis was given to: antennae, palps, cirri on segment 1, dorsal cirri on segment 2, dorsal cirri  
286 of median segments and ventral cirri of median segments.

287 All measurements were done with a LEICA MC170 HD stereo microscope, with an  
288 incorporated measurement software. Supplementary Table S2 shows detailed morphometric  
289 values for each specimen.

290

## 291 RESULTS

292

### 293 PHYLOGENY RECONSTRUCTION

294 The BI phylogenetic trees (Fig. 2A, B) were created from a dataset of 297 COI, 94 16S,  
295 192 ITS, and 28S sequences belonging to specimens of the *Essc* and four outgroup species (*E.*  
296 *bahusiensis*, *E. ockelmanni*, *S. fusigera*, and *E. aff. ockelmanni*). Support values over 0.85 are  
297 shown in the BI trees. Since BI and ML trees display a different topology, ML bootstrap values  
298 are not shown in the BI tree. Detailed ML trees with 1 000 bootstrap support values, for both  
299 mitochondrial and nuclear concatenated datasets, are available in the supplementary material  
300 (Fig. S1 and Fig. S2, respectively).

301 Both mitochondrial and nuclear loci showed evidence of at least five new *Eumida* MOTUs  
302 compared to the previous studies, with mitochondrial markers also revealing a distinct British  
303 MOTU close to *E. merope*, hereafter referred to as *E. aff. merope* (MOTU 11, Fig. 2A); a new  
304 Mediterranean MOTU close to *E. kelaino*, hereafter referred to as *E. aff. kelaino* (MOTU 17, Fig.  
305 2A); another British MOTU close to *E. gretathunbergae* sp. nov., hereafter referred to as *E. aff.*  
306 *gretathunbergae* (MOTU 13, Fig. 2A); and lastly an additional unnamed Italian lineage *Eumida*  
307 ORB997 (MOTUs 2 and 23, Fig. 2A, B) close to the new species *E. pleijeli* sp. nov.

308 Apart from outgroups, the number of consensus MOTUs ranged between 18 (Fig. 2B)  
309 and 22 (Fig. 2A). Most of them were present either in Great Britain, Scandinavia, or southern  
310 France. The newly described species, *Eumida gretathunbergae* sp. nov., was present in the  
311 British Isles and northern France (MOTU 12 and 25, Fig. 2A, B); *E. pleijeli* sp. nov. (MOTUs 3 and  
312 23, Fig. 2A, B) and *E. langenecki* sp. nov. (MOTUs 5, Fig. 2A, B) were both in Western Italy; *E.*  
313 *schanderi* sp. nov. [previously referred to as *Eumida* unnamed species S21 from Nygren & Pleijel  
314 (2011)] exclusively in Norway and Sweden (MOTUs 22 and 26, Fig. 2A, B); and lastly *E. fenwicki*  
315 sp. nov. [previously named *Eumida* unnamed species GB22 from Teixeira *et al.* (2020)] in both  
316 Scandinavia and Great Britain (MOTU 6, Fig. 2A, B).

317 The closely related species *E. notata* (MOTU 9, Fig. 2A) and *E. merope* (MOTU 10, Fig.  
318 2A), including the new British lineage *E. aff. merope* (MOTU 11, Fig. 2A), could be completely  
319 sorted using mitochondrial loci, forming highly supported clades in the BI tree. However, only one



320 of the clustering algorithms could split these lineages into three distinct MOTUs by using nuclear  
321 markers, with the remaining ones being clustered together in a low supported monophyletic clade  
322 instead (MOTU 24, Fig. 2B). A similar pattern was also observed between *Eumida pleijeli* sp. nov.  
323 and *Eumida* ORB997 (MOTU 23, Fig. 2B), between *E. aff. gretathunbergae* and *E. gretathunbergi*  
324 sp. nov. (MOTU 25, Fig. 2B), and between *E. aff. kelaino* and *E. kelaino* (MOTU 27, Fig. 2B).

325 Distinct marker-dependent MOTU sorting cases were also observed for *E. schanderi* sp.  
326 nov., in which MOTU 26 was delimited only with nuclear markers. This sorting is recorded  
327 independently for both ITS and 28S, as evidenced in the haplotype networks detailed further  
328 below.

329

### 330 GENETIC DISTANCES AND *EUMIDA* AFF. *OCKELMANNI*

331 Assuming *E. aff. merope*, *E. aff. kelaino*, and *E. aff. gretathunbergae* as valid species,  
332 the global mean genetic distances for the whole *complex* can be found in Table 2, including the  
333 distances of the most similar and divergent MOTUs for the nearest and farthest neighbours,  
334 respectively. The mean intraspecific distances were 0.59 (0 – 3.8) % for COI and 0.18 (0 – 0.8)  
335 % for 16S, while average congeneric distances are 16.7 (5.5 – 23.4) % and 7.6 (0.3 – 15.1) %  
336 respectively. The distances for ITS-region ranged between 0.44 (0 – 5.8) % and 9.2 (0.5 – 18.1)  
337 % for intra- and interspecific divergence, respectively, whereas for 28S, the corresponding  
338 distances were 0.06 (0 – 0.8) % and 1.7 (0 – 4.5) %, respectively. The two MOTUs found in *E.*  
339 *schanderi* were responsible for the high intraspecific maximum distances reported for the nuclear  
340 loci.

341 At first, *E. aff. ockelmanni* was assigned to the *Essc* based on morphological similarity;  
342 however, genetic distances and BI phylogenetic tree topology signalled otherwise. The two  
343 available specimens were very small (less than 2 mm), which can sometimes lead to  
344 misidentifications in *Eumida*. Upon a more careful morphological analysis, we concluded that this  
345 MOTU is closer to the outgroup belonging to *E. ockelmanni*. This seems to corroborate the  
346 molecular data, in which we observed unusually high molecular distances compared to the  
347 remaining *Essc*. This is true especially regarding nuclear markers (maximum distances up to 38.2  
348 and 9.7% for ITS region and 28S, respectively), and yet much closer to *E. ockelmanni* (maximum  
349 distances up to 13.8 and 1.8% for ITS region and 28S, respectively), which might indicate a  
350 species complex still undescribed for this group as well.

351

### 352 HAPLOTYPE NETWORKS

353 All haplotype networks (COI, Fig. 3; ITS, 28S, 16S, Fig. 4A-C) show that the five new  
354 species, as well as the new unnamed *Eumida* lineages, are completely sorted from each other  
355 and the remaining *Essc*. This is even observed in 28S haplotypes (Fig. 4B), which is a slowly  
356 evolving gene and may fail to exhibit complete classification when others do, especially when  
357 dealing with closely related species. The only exception to this pattern is observed in the  
358 Mediterranean and British lineages from *E. merope* and *E. aff. merope*, which shared haplotypes  
359 both in 28S and ITS loci. The low number of mutational steps between nuclear haplotypes, such

360 as evidenced in the ITS and 28S networks (Fig. 4A, B), may be responsible for their lower  
361 phylogenetic resolution when it comes to delineating MOTUs 23, 24, 25, and 27 (Fig. 2B). All of  
362 the MOTUs were sympatric with at least one other MOTU within the *Essc*, except the MOTUs  
363 from Italy and *E. notata*.

364 Additionally, two distinct ITS and 28S haplotypes for *E. schanderi* sp. nov. were found,  
365 which correspond to different MOTUs in the BI tree (22 and 26, Fig. 2B). Also, two distinct groups  
366 of haplotypes for *E. alkyone* could be distinguished based on ITS alone, in which no sharing is  
367 observed between Norwegian and Swedish specimens. Three completely sorted COI haplotype  
368 groups were also found within *E. taygete*, splitting the Mediterranean and British populations and  
369 adding a unique shared haplotype in samples from both regions, with seven mutations apart from  
370 the remaining ones.

371 No MOTU has a central position from which every other derived in any of the networks,  
372 and a large amount of circular COI mutation paths are found mainly in *E. notata*, *E. sanguinea*  
373 s.s., *E. alkyone*, *E. merope*, and *E. aff. merope*.

374 Haplotype diversity within the *Essc* is relatively high for COI (Table 3), with *E. fenwicki*  
375 sp. nov., *E. mackiei*, and *E. maia* being the only ones with significant negative Tajima D or Fu and  
376 Li's D tests. Therefore, the population might be in expansion after a recent bottleneck or linkage  
377 to a swept gene, with the neutral model of nucleotide substitutions being accepted for the  
378 remaining MOTUs. *Eumida mackiei* and *E. gretathunbergi* sp. nov. have the highest haplotype  
379 diversity (HD [COI]: 0.99) and segregating sites (S= 37 and 39 respectively).

380

#### 381 LIVE PHOTOGRAPHS AND PIGMENTATION DATA

382 A summary of the different white pigmentation combinations [types A to H, following  
383 Nygren & Pleijel (2011)] observed for all the species in the complex is given in Table 4. Live  
384 photographs of specimens exhibiting white pigmentation patterns and colour, belonging to the  
385 newly described species and unnamed *Eumida* lineages (RO174-180, ANT002, and ORB997),  
386 including *E. aff. merope*, *E. aff. kelaino* and *E. aff. gretathunbergae* can be found in Fig. 5A-F,  
387 Fig. 6A-E and Fig. 7A-C. Three of the five new species (*E. schanderi* sp. nov., *E. fenwicki* sp.  
388 nov., and *E. gretathunbergae* sp. nov.) share type B pigmentation, which corresponds to the  
389 absence of white pigmentation. However, *E. schanderi* sp. nov. (Fig. 5A) and *E. gretathunbergae*  
390 sp. nov. (Fig. 5D) are polymorphic, with some specimens also exhibiting type D (dorsally on  
391 segment 2 only, Fig. 5B) and F (Fig. 5C) pigmentation, respectively (see Table 4). Type F  
392 pigmentation was defined by Nygren & Pleijel (2011) as a single longitudinal line of white  
393 pigmentation and erroneously assigned to one specimen designated as *Eumida* unnamed  
394 species S21, here named as *E. schanderi* sp. nov. This specimen presents type B pigmentation,  
395 i.e., no white pigmentation. Type F pigmentation is here redefined as white transverse dorsal lines  
396 present on most segments. *Eumida fenwicki* sp. nov. also possesses type B pigmentation (Fig.  
397 5E), while *E. pleijeli* sp. nov. (Fig. 6D) has a green colour with type C, characterized by the  
398 presence of a longitudinal white line together with white pigmentation dorsally on segment 2.

399 Two other pigmentation types are newly defined in this study, namely: type G, with white  
400 pigmentation from the prostomium to the middle of the eyes of worms, similar to type E, but with  
401 the addition of small dorsal transverse white dots, which seems to be unique to *E. langenecki* sp.  
402 nov. (Fig. 6C); and type H, spotted in the currently unnamed *Eumida* ORB997 (Fig. 6E), defined  
403 by the presence of white pigmentation dorsally on segment 2 but with a non-white eye-like pattern  
404 dorsally between segments along the whole body of the worm. *Eumida* ORB997 has a very  
405 distinct pigmentation among all members of the *Essc*, including *E. pleijeli* sp. nov., even though  
406 these two species share the same nuclear MOTU.

407 *Eumida* aff. *merope* is also polymorphic and shares the same type D (Fig. 6B) and A (Fig.  
408 6A) white pattern as the Mediterranean counterpart. *Eumida* aff. *gretathunbergae* possesses  
409 both type B and F (Fig. 7C) pigmentation types, following the same pattern as its sister lineage  
410 *E. gretathunbergae* sp. nov.. *Eumida* aff. *kelaino* has type C (Fig. 7B) similar to *E. kelaino*, while  
411 the unnamed *Eumida* RO174-180 has type B (Fig. 5F) and lastly the unnamed *Eumida* ANT002  
412 (Fig. 7D) has type D. The new British *E. taygete* population has an additional pigmentation (type  
413 B) compared to the Mediterranean populations (type D). *E. elektra* population from northern  
414 France also has a distinct pigmentation (type D) when compared to the Scandinavian populations  
415 (type B). Apart from *E. schanderi* sp. nov., *E. elektra*, *E. merope*, *E. aff. merope*, *E. taygete*, *E.*  
416 *gretathunbergae* sp. nov., and *E. aff. gretathunbergae*, the remaining lineages of the *Essc* only  
417 have a single pigmentation type as far as we know.

418 In total, the *Essc* is composed of eight variable pigmentation types distributed among 22  
419 distinct COI clades. Based on geographic distribution and pigmentation types, *Essc* belonging  
420 species can be significantly narrowed down without using molecular data, distinguishing some  
421 only based on these criteria (see the *Essc* key in the taxonomic section).

422

#### 423 MORPHOMETRIC MEASUREMENTS

424 The different morphometric proportions seen in the scatter plots in Fig. 8A-H are the only  
425 ones displaying significant visible differences, with the formation of independent clusters among  
426 the analysed MOTUs. A variation of either nine or ten specimens per lineage were analysed. The  
427 use of morphometric proportions of antenna length (AL) against head length or width (HL; HW),  
428 palp length (PL), cirri on segment 1 or dorsal cirri on segment 2 (CS1L; DCS2L), and median  
429 antenna length (MAL) seems to be effective in distinguishing *E. gretathunbergae* sp. nov., *E.*  
430 *schanderi* sp. nov., *E. fenwicki* sp. nov., and *E. elektra* from each other (main morphometric  
431 findings summarized in Table 5). The larger number of segments and worm length is also very  
432 distinct in *E. gretathunbergae* sp. nov. (Fig. 8G, H). The short antennal length recorded for one  
433 of the *E. elektra* specimens (around 0.158 mm), which might be due to damages during sampling,  
434 could be the reason for the overlap with the remaining analysed species. Even though there are  
435 not enough available specimens to form morphometric clusters for *Eumida pleijeli* sp. nov. and *E.*  
436 *langenecki* sp. nov., these species can still be described with unique features that distinguish  
437 them from the remaining *Essc*. To do so, a combination of pigmentation type, live colouration,

438 and geographic range (Table 5) is needed and complemented with the molecular data seen above  
439 (Fig. 2).

440 As for finding possible morphometric variations between the sister lineages *E. merope*  
441 and *E. aff. merope*, our results (Fig. 9A-F) reveal high intraspecific variation within *E. aff. merope*,  
442 whose morphometric measurements are scattered around the other analysed species for most of  
443 the proportions, except when comparing antennae (AL) and palp (PL) lengths (Fig. 9B). Some  
444 partial overlaps between *E. notata* and *E. merope* are also observed. However, *E. merope*, *E.*  
445 *schanderi* sp. nov., and *E. gretathunbergae* sp. nov. seem to have palps longer than antennae.  
446 This is contrary to the remaining species analysed in ours or other previous studies, which either  
447 have antennae larger than palps or of the same proportion. Besides AL/PL ratio, *E. notata* can be  
448 differentiated from *E. elektra*, *E. merope*, and *E. aff. merope* by comparing worm width (WW) with  
449 worm width with parapodia (WWP) (Fig. 9A). Some morphometric clusters may also overlap with  
450 *E. elektra*, probably due to how genetically close this species is against the remaining analysed  
451 ones. Moreover, the mean COI distances between this species and the closest neighbours are  
452 shared with *E. notata*, *E. aff. merope*, and *E. alkyone*, with K2P values of 13.8, 13.5, and 12.6 %,  
453 respectively.

454 A detailed description of the five new species can be found in the taxonomic section  
455 below, with their respective Zoobank Isid registration codes.

456

## 457 TAXONOMY

458

### 459 *Eumida sanguinea* species complex (Essc)

460

461 *Diagnosis* (amended from Nygren & Pleijel, 2011)

462 *Eumida* with cordate dorsal cirri, near-symmetrical along the longitudinal axis, 1.25–1.9  
463 times longer than wide. Colour varies between light yellow, yellowish-brown and green, distributed  
464 among eight different pigmentation types (Table 4). Small to medium-sized worm, usually  
465 between 3 to 30 mm in length and 30 to 110 segments. High intraspecific morphometric variation.

466

#### 467 *Remarks*

468 *Eumida sanguinea* species complex is an informal name for a clade that includes fifteen  
469 described species in north-east Atlantic waters (Nygren & Pleijel 2011; Teixeira *et al.* 2020)  
470 including the new ones described herein, with an addition of four undescribed lineages (*Eumida*  
471 F22, RO174-180, ANT002, and ORB997) and three distinct mitochondrial sister lineages (*E. aff.*  
472 *merope*, *E. aff. kelaino*, and *E. aff. gretathunbergae*). This designation should be applied for  
473 identifications based on the morphology of preserved specimens, in which white pigmentation  
474 has disappeared and no molecular data is available.

475 Recorded egg sizes are 85–95 µm for specimens from Danish waters (Eibye-Jacobsen,  
476 1991) and 90 µm for specimens from the English Channel and Sweden (Pleijel, 1993). Egg sizes  
477 up to 110 µm were also observed by Nygren & Pleijel (2011) for some members of the complex.

478 Cazaux (1970) described the development from trochophore to newly settled stages from  
479 Bordeaux in France.

480 *Eumida bahusiensis* Bergstrom, 1914 is phylogenetically very close to *Essc* species and  
481 can therefore be part of it. The species can be distinguished morphologically by its broader dorsal  
482 and ventral cirri distally pointed and by the green colour with white type A pigmentation in live  
483 animals (Nygren *et al.* 2017). However, it can often be confused with *Eumida mackiei* (Teixeira,  
484 Nygren and Pleijel, 2020), which has the same background colour and pigmentation, as well as  
485 median ventral cirri, approaching the broader form of *E. bahusiensis*. The two species are  
486 genetically very distinct with 21% COI average divergence and are not sister species.

487

488 A simple *Essc* key based on pigmentation types and geographic distribution can be seen  
489 below. This key should only be used for identifications where pigmentation and colour of live  
490 specimens were recorded. Table 4 displays the pigmentation types.

491

492 **1) Scandinavia**

493 a) Type A pigmentation.....*E. alkyone*

494 b) Type B pigmentation

495 b1) Palps longer than antennae.....*E. schanderi*

496 b2) Palps shorter than antennae.....*E. elektra*, *E. fenwicki*

497 (The distinction between these two species is only possible with molecular data)

498 c) Type C pigmentation .....*E. kelaino*

499 d) Type D pigmentation ..... *E. sanguinea* s.s., *E. schanderi*

500 (The distinction between these two species is only possible with molecular data)

501

502 **2) Great Britain + Brittany, France**

503 a) Type A pigmentation

504 a1) Greenish colour

505 a1.1) Palps as long as antennae .....*E. mackiei*

506 a1.2) Palps shorter than antennae .....*E. maia*

507 a2) Yellowish-brown colour

508 a2.1) Palps longer than antennae ..... *E. gretathunbergae*; *E. aff. gretathunbergae*;

509 (The distinction between these two species is only possible with molecular data)

510 a2.2) Palps shorter than antennae .....*E. aff. merope*

511 b) Type B pigmentation .....*E. taygete*, *Eumida* RO174-180, *E. fenwicki*

512 (The distinction between these three species is only possible with molecular data)

513 c) Type C pigmentation .....*E. kelaino*

514 d) Type D pigmentation .....*E. sanguinea* s.s., *E. elektra*; *E. aff. merope*

515 (The distinction between these three species is only possible with molecular data)

516 e) Type F pigmentation ..... *E. gretathunbergae*; *E. aff. gretathunbergae*

517 (The distinction between these two species is only possible with molecular data)

518

519 **3) Madeira Island (Portugal)**

520 a) Type E pigmentation .....*E. notata*

521

522 **4) Western Mediterranean**

523 a) Type A pigmentation ..... *E. maia*

524 b) Type B pigmentation ..... *E. asterope*

525 c) Type C pigmentation

526 c1) Green colour.....*E. pleijeli*

527 c2) Yellowish colour.....*E. aff. kelaino*

528 d) Type D pigmentation ..... *E. merope*, *Eumida* F22, *E. taygete*; *Eumida* ANT002

529 (The distinction between these four species is only possible with molecular data)

530 e) Type G pigmentation ..... *E. langenecki*

531 f) Type H pigmentation ..... *Eumida* ORB997

532

533 **5) Eastern Mediterranean**

534 a) Type A pigmentation ..... *E. merope*

535 b) Type D pigmentation ..... *E. taygete*

536

537

538

***Eumida fenwicki* sp. nov.**

539

urn:lsid:zoobank.org:act: DA689D94-E20B-4126-8DA4-575576EB5C86

540

541 *Material examined*

542 *Type material.* Great Britain, Cornwall: 1 spm, holotype and hologenophore,  
543 DBUA0002396.01, 50°21.5'N, 04°08.9'W, 10m, coarse shell gravel, dredge, 16-03-2011; 1 spm,  
544 paratype and paragenophore, DBUA0002396.02, 50°21.5'N, 04°08.9'W, 10m, coarse shell  
545 gravel, dredge, 16-03-2011. The type specimens were collected by David Fenwick.

546 *Other material.* Great Britain, Cornwall: 5 spms, DBUA0002397.01-05, 50°06'12.0"N,  
547 5°32'49.4"W, pontoon scrapings, 14/04/2015, 02/04/2015, 04/05/2015, 07/05/2015 and  
548 28/05/2015 respectively; 1spm, DBUA0002397.06, 50°06'12.0"N, 5°32'49.4"W, pontoon  
549 scrapings, 13/07/2016; Norway, Agdenes: 9 spms, ZMBN\_134523 - 134530; DBUA0002398.01,  
550 63°35.721'N, 9°33.100'E, 10m, sand, shell-fragments, dredge, 05/09/2016; 3 spms,  
551 ZMBN\_134531 - 134533, 63°35.721'N, 9°33.100'E, 2m, coarse gravel and rocks, dredge,  
552 05/09/2016; France, Roscoff: 2 spms, DBUA0002399.01-02, 48°44'55.2"N, 3°54'23.3"W, 45m,  
553 gravel, 01/02/2018. British specimens were collected by David Fenwick, while the Norwegian  
554 ones were collected by the students from the ForBio programme. All specimens are preserved in  
555 ethanol 96%. The specimens from Norway are deposited at the University Museum of Bergen  
556 (ZMBN), and the remaining ones, including the holotype and paratype, at the Biological Research

557 Collection (Marine Invertebrates) of the Department of Biology of the University of Aveiro (COBI  
558 at DBUA), Portugal.

559

560 *Diagnosis*

561 Member of *Essc* with type B pigmentation (Table 4), i.e., without white pigmentation (Fig.  
562 5E). Live specimens present light-yellowish colouration. Antennae slightly longer than palps.  
563 Proportions between antenna length and cirri length on segment 1, dorsal cirri length on segment  
564 2, or head length and width smaller than those found in *E. gretathunbergae* sp. nov. and *E. elektra*,  
565 but greater than those of *E. schanderi* sp. nov. Palp length, cirri on segment 1 and dorsal cirri on  
566 segment 2, and head length and width are considerable smaller when compared to the same  
567 length of *E. gretathunbergae* sp. nov. antennae. Dorsal cirri on segment 2 usually twice as long  
568 as cirri on segment 1. Head wider rather than longer. Dorsal cirri of median segments 1.5 times  
569 longer rather than wider. Ventral cirri of median segments twice as long rather than wider.  
570 Proboscis not observed. Worms small, usually between 3 to 10 mm long, with 45 to 75 segments.

571

572 *Molecular data*

573 COI, 16S, ITS, and 28S sequences as in specimens DBUA0002396.01-06;  
574 ZMBN\_134523 to 134533; DBUA0002398.01; DBUA0002399.01-02 (Table S1). Phylogenetic  
575 relationship as in Fig. 2A-B, with high support values and low intraspecific (<3%) genetic  
576 divergence for both mitochondrial and nuclear markers. Mean interspecific COI distances to the  
577 nearest and farthest neighbours are 14.8% (K2P, *E. aff. merope*) and 21.1% (K2P, *E. schanderi*  
578 sp. nov.), respectively. DOI for the species' Barcode Index Number (BIN):  
579 dx.doi.org/10.5883/BOLD:ADG3938.

580

581 *Etymology*

582 The new species is named after David Fenwick to recognize his kindness in collecting  
583 and photographing a large number of *Eumida* specimens on the behalf of the last author of this  
584 paper.

585

586 *Distribution and habitat:*

587 Atlantic Ocean – from Norway to the British Isles, 2 to 10 m depth, on coarse gravel and  
588 rocks.

589

590 *Remarks*

591 Morphologically similar to *E. sanguinea sensu stricto* (Örsted, 1843), except for  
592 pigmentation pattern. Pigmentation type B shared with *E. asterope* Nygren & Pleijel, 2015; *E.*  
593 *elektra* Nygren & Pleijel, 2015; some specimens of *E. schanderi* sp. nov.; the British population  
594 of *E. taygete* Nygren & Pleijel, 2011; *Eumida* RO174-18; and some specimens from *E.*  
595 *gretathunbergae* sp. nov. and *E. aff. gretathunbergae*. However, those species differ from *E.*  
596 *fenwicki* sp. nov. at the molecular level, with mean interspecific COI distances (K2P, %) of 19.4,

597 15.1, 21.1, 17.3, 17.7, 16.6, and 16.5 respectively. Morphometric proportions of the antennal  
598 length against either head length or width, palp length, cirri on segment 1, and dorsal cirri on  
599 segment 2 seem to be effective in distinguishing this species from *E. gretathunbergae*, *E.*  
600 *schanderi*, and *E. elektra*.

601

602 ***Eumida schanderi* sp. nov.**

603 urn:lsid:zoobank.org:act: 4780C5B7-EC23-44A5-B2CC-88E9FE8C5891

604

605 *Material examined*

606 *Type material.* Norway, Bergen: 1 spm, holotype and hologenophore, ZMBN\_134556,  
607 60°14'11.9"N, 5°12'02.1"E, 27m, algae, gravel, triangular dredge, 24/07/2014; 11 spms,  
608 paratypes and paragenophores, ZMBN\_134550 - 134555; ZMBN\_134557 - 134561,  
609 60°14'11.9"N, 5°12'02.1"E, 27m, algae, gravel, triangular dredge, 24/07/2014. The type  
610 specimens were collected by the crew aboard R/V Hans Brattström owned by the University of  
611 Bergen and operated by the Institute of Marine Research.

612 *Other material.* Sweden, Bohuslän: 1spm, SMNH 110614, 58°52'00.0"N, 11°06'00.0"E,  
613 40m, gravel, dredge, 12/05/2005. Collected by Fredrik Pleijel. All specimens, including the  
614 holotype and paratypes, are preserved in ethanol 96% and deposited at the University Museum  
615 of Bergen (ZMBN), with the exception of the Swedish one, which is deposited in the Swedish  
616 Museum of Natural History (SMNH).

617

618 *Diagnosis*

619 Member of *Essc* with type D pigmentation (Table 4), i.e., with white pigmentation present  
620 dorsally on segment 2 and anterior cirri (Fig. 5B). Type B pigmentation, i.e., without white  
621 pigmentation (Fig. 5A) also observed in some paratypes and other analysed material. Live  
622 specimens present greenish colouration. Antennae slightly shorter than palps. Proportions  
623 between the antenna length and head length or width, median antenna length, cirri on segment  
624 1, and dorsal cirri on segment 2 smaller than those in *E. gretathunbergae* sp. nov., *E. fenwicki* sp.  
625 nov., and *E. elektra*. Palp length, cirri on segment 1, and dorsal cirri on segment 2, or head width  
626 similar to those of *E. fenwicki*. Head almost twice as wide as long. Dorsal cirri on segment 2  
627 usually twice as long as cirri on segment 1. Dorsal cirri of median segments very large, almost  
628 twice as long rather than wider. Ventral cirri of median segments longer rather than wider, usually  
629 twice as long. Proboscis with numerous minute papillae evenly distributed (Fig. 5B). Worms small,  
630 usually between 3 to 7 mm long, with 40 to 60 segments.

631

632 *Molecular data*

633 COI, 16S, ITS, and 28S sequences as in specimens ZMBN\_134550 to 134561 and  
634 SMNH 110614 (Table S1). Phylogenetic relationship as in Fig. 2A, B, with high support values  
635 and low intraspecific (<3%) genetic divergence for mitochondrial loci. However, introgression of  
636 mtDNA from a non-sampled lineage may be present in nuclear markers with two strongly-



637 supported sister MOTUs with 5.8 and 0.6% mean genetic divergence for ITS and 28S,  
638 respectively. Mean interspecific COI distances to the nearest and farthest neighbours are 15.6%  
639 (K2P, *E. aff. merope*) and 21.8% (K2P, *E. langenecki* sp. nov.), respectively. DOI for the species'  
640 Barcode Index Number (BIN): dx.doi.org/10.5883/BOLD:ACQ6378.

641

642 *Etymology*

643 The new species is named to honour the memory of Christoffer Schander (1960-2012),  
644 a much-appreciated former colleague to the last author of this paper.

645

646 *Distribution and habitat:*

647 Atlantic Ocean – Norway and Sweden, from 27 to 40 m depth, on gravel with algae.

648

649 *Remarks*

650 Morphologically similar to *E. sanguinea sensu stricto* (Örsted, 1843), including  
651 pigmentation pattern. Pigmentation type D shared with *E. sanguinea* s.s.; *E. merope* Nygren &  
652 Pleijel, 2015; *E. aff. merope*; *Eumida* F22 Nygren & Pleijel, 2011; *Eumida* ANT002; and the  
653 Mediterranean population of *E. taygete* Nygren & Pleijel, 2011. Pigmentation type B shared with  
654 *E. fenwicki* sp. nov.; *E. asterope* Nygren & Pleijel, 2011; *E. elektra* Nygren & Pleijel, 2011; *E.*  
655 *gretathunbergae* sp. nov.; and the British population of *E. taygete* Nygren & Pleijel, 2011.  
656 However, those species differ from *E. schanderi* at the molecular level, with mean interspecific  
657 COI distances (K2P, %) of 15.1, 17.3, 15.6, 18.6, 16.5, 21.1, 16.5, 18.8, and 18.4, respectively.  
658 Proboscis has papillae (Fig. 5B), unlike the one reported in *E. sanguinea* s.s., which is almost  
659 smooth with sparsely distributed minute papillae, arranged in six more-or-less distinct rows  
660 (Pleijel, 1993). Morphometric proportions of the antenna-palp ratio and antenna length against  
661 head length or width, palp length, cirri on segment 1, and dorsal cirri on segment 2, and median  
662 antenna seem to be effective in distinguishing this species from *E. gretathunbergae* sp. nov., *E.*  
663 *schanderi* sp. nov., and *E. elektra*.

664

665 ***Eumida gretathunbergae* sp. nov.**

666 urn:lsid:zoobank.org:act:B974C7EA-E00D-4D8A-B791-5A82BAEAAADE

667

668 *Material examined*

669 *Type material.* Great Britain, Plymouth: 1 spm, *holotype and hologenophore*,  
670 DBUA0002400.01, 50°21'30.0"N, 4°08'54.0"W, 15m, coarse shell gravel, dredge, 16/03/2011; 8  
671 spms, paratypes and paragenophores, DBUA0002400.02-09, 50°21'30.0"N, 4°08'54.0"W, 15m,  
672 coarse shell gravel, dredge, 16/03/2011. Collected by the crew aboard R/V SEPIA (Marine  
673 Biological Association) and Fredrik Pleijel.

674 *Other material.* Great Britain, Plymouth: 17 spms, DBUA0002400.10-26, 50°21.59"N,  
675 4°09.03"W, 8 - 13m, coarse shell gravel, dredge, 27/03/2017. Collected by the crew aboard R/V  
676 SEPIA (Marine Biological Association) and Fredrik Pleijel. All specimens, including the holotype

677 and paratypes, are preserved in ethanol 96% and deposited at the Biological Research Collection  
678 (Marine Invertebrates) of the Department of Biology of the University of Aveiro (COBI at DBUA),  
679 Portugal.

680

#### 681 *Diagnosis*

682 Member of *Essc* with type F pigmentation (Table 4), i.e., with transverse dorsal lines  
683 across segments (Fig. 5C). Type B pigmentation, i.e., without white pigmentation (Fig. 5D) also  
684 observed in some paratypes and other analysed material. Live specimens present yellowish-  
685 brown colouration. Antennae are shorter than palps. Proportions of the antenna length against  
686 head length or width, median antenna length, cirri on segment 1, and dorsal cirri on segment 2  
687 larger than those of *E. schanderi* sp. nov. and *E. fenwicki* sp. nov., but smaller than those of *E.*  
688 *elektra*. Despite a significantly larger worm size, antenna length with similar morphometric  
689 measurements as *E. fenwicki* sp. nov. Head wider than longer. Dorsal cirri on segment 2 usually  
690 twice as long as cirri on segment 1. Dorsal cirri of median segments large, 1.5 times longer rather  
691 than wider. Ventral cirri of median segments twice longer than wider. Proboscis with numerous  
692 minute papillae evenly distributed (Fig. 5C). Worms small- to medium-sized, usually between 10  
693 to 20 mm long, with 80 to 105 segments.

694

#### 695 *Molecular data*

696 COI, 16S, ITS, and 28S sequences as in specimens DBUA0002400.01-26 (Table S1).  
697 Phylogenetic relationship as in Fig. 2A, B, with high support values and low intraspecific (<3%)  
698 genetic divergence for both mitochondrial and nuclear markers. Mean interspecific COI distances  
699 to the nearest and farthest neighbours are 13% (K2P, *E. aff. gretathunbergae*) and 21.8% (K2P,  
700 *Eumida* ORB997), respectively. DOI for the species' Barcode Index Number (BIN):  
701 [dx.doi.org/10.5883/BOLD:AEA3142](https://dx.doi.org/10.5883/BOLD:AEA3142).

702

#### 703 *Etymology*

704 The new species is named after Greta Thunberg to honour her achievement in gathering  
705 attention from the general public towards climate change.

706

#### 707 *Distribution and habitat:*

708 Atlantic Ocean – British Isles, 8-15 m depth, on coarse shell gravel.

709

#### 710 *Remarks*

711 Morphologically similar to *E. sanguinea sensu stricto* (Örsted, 1843), except for  
712 pigmentation pattern. Type F pigmentation is unique for this species (including *E. aff.*  
713 *gretathunbergae*). Type B pigmentation is shared with *E. fenwicki* sp. nov.; *E. asterope* Nygren &  
714 Pleijel, 2011; *E. elektra* Nygren & Pleijel, 2011; *E. aff. gretathunbergae*; *Eumida* RO174-180;  
715 some specimens of *E. schanderi* sp. nov.; and the British population of *E. taygete* Nygren &  
716 Pleijel, 2011. However, those species differ from *E. gretathunbergae* sp. nov. at the molecular

717 level, with mean interspecific COI distances (K2P, %) of 16.6, 15.5, 16.6, 13.0, 14.5, 18.4, and  
718 16.0, respectively. Proboscis has papillae (Fig. 5C), unlike the one reported in *E. sanguinea* s.s.,  
719 which is almost smooth with sparsely distributed minute papillae, arranged in six more-or-less  
720 distinct rows (Pleijel, 1993). The number of segments, worm length, antennae/palps ratio, as well  
721 as morphometric proportions of the antenna length against head length or width, palp length, cirri  
722 on segment 1, dorsal cirri on segment 2, and median antenna, seem to be very effective in  
723 distinguishing this species from *E. fenwicki* sp. nov., *E. schanderi* sp. nov., and *E. elektra*.

724

725 ***Eumida pleijeli* sp. nov.**

726 urn:lsid:zoobank.org:act: F2B43974-0771-4B9A-9CC9-42FF33CEB454

727

728 *Material examined*

729 *Type material.* Italy, Naples: 1 spm, holotype and hologenophore, DBUA0002407.02,  
730 40°49'48.0"N, 14°14'13.2"E, 6m, coarse shell gravel, dredge, 05/05/2010; 1 spm, paratype and  
731 paragenophore, DBUA0002407.01, 40°49'48.0"N, 14°14'13.2"E, 6m, coarse shell gravel, dredge,  
732 05/05/2010. Collected by Joachim Langeneck.

733 All type specimens are preserved in ethanol 96% and deposited at the Biological  
734 Research Collection (Marine Invertebrates) of the Department of Biology of the University of  
735 Aveiro (COBI at DBUA), Portugal.

736

737 *Diagnosis*

738 Member of *Essc* with green colouration mixed with type C pigmentation (Table 4), i.e.,  
739 white pigmentation dorsally on segment 2 and anterior cirri, and with a longitudinal mid-dorsal line  
740 (Fig. 6D). Antennae longer than palps. Dorsal cirri on segment 2 almost three times as long as  
741 cirri on segment 1, unlike the smaller ratio (twice as long) in *E. fenwicki* sp. nov., *E. schanderi* sp.  
742 nov, *E. gretathunbergae* sp. nov. *E. langenecki* sp. nov. and *E. elektra*. Dorsal cirri of median  
743 segments large, 1.5 times longer rather than wider, with similar ratio as *E. fenwicki* sp. nov., *E*  
744 *gretathunbergae* sp. nov. *E. langenecki* sp. nov. and *E. elektra*, but smaller than *E. schanderi* sp.  
745 nov. (usually twice as long). Ventral cirri of median segments 1.5 times longer rather than wider,  
746 but with smaller ratio (usually twice as long) as *E. fenwicki* sp. nov., *E. schanderi* sp. nov, *E*  
747 *gretathunbergae* sp. nov. *E. langenecki* sp. nov. and *E. elektra*. Proboscis not observed. Worms  
748 small- to medium-sized, usually between 10 to 15 mm long, with 55 to 65 segments.

749

750 *Molecular data*

751 COI, 16S, ITS, and 28S sequences as in specimens DBUA0002407.01-02 (Table S1).  
752 Phylogenetic relationship as in Fig. 2A, B, with high support values and low intraspecific (<3%)  
753 genetic divergence for both mitochondrial and nuclear markers. However, nuclear markers (ITS  
754 and 28S) group this species into the same MOTU as the unnamed *Eumida* ORB99, even though  
755 high interspecific COI divergence is found (18%, K2P). Mean interspecific COI distances to the  
756 nearest and farthest neighbours are 16.8% (K2P, *E. mackiei*) and 21.6 (K2P, *E. langenecki* sp.

757 nov.), respectively. DOI for the species' Barcode Index Number (BIN):  
758 [dx.doi.org/10.5883/BOLD:AEH2033](https://dx.doi.org/10.5883/BOLD:AEH2033)

759

760 *Etymology*

761 The new species is named after Fredrik Pleijel to honour his passion and dedication to  
762 the study of the Phyllodocidae.

763

764 *Distribution and habitat:*

765 Western Mediterranean Sea – Italy, 6 m depth, on coarse shell gravel.

766

767 *Remarks*

768 Morphologically similar to *E. sanguinea sensu stricto* (Örsted, 1843), except for  
769 pigmentation pattern. Type C pigmentation is shared only with *E. kelaino* and its Mediterranean  
770 counterpart *E. aff. kelaino*. However, *E. kelaino* and *E. aff. kelaino* differ greatly from *E. pleijelii*  
771 sp. nov. at the molecular level, with mean interspecific COI distances (K2P, %) of 19.0 and 19.1,  
772 respectively, and share a different colouration. This species can share the same nuclear MOTU  
773 (ITS+28S) as the unnamed *Eumida* ORB997, but the latter has a very distinct pigmentation (Type  
774 H) among all members of the *Essc*. *E. pleijelii* sp. nov. can be identified based only on colour,  
775 pigmentation, and geographic distribution jointly.

776

777

***Eumida langenecki* sp. nov.**

778

urn:lsid:zoobank.org:act: 3E870E7A-C1D6-4918-BCE0-737E5B81418A

779

780 *Material examined*

781 *Type material.* Italy, Antignano: 1 spm, holotype and hologenophore, DBUA0002409.02,  
782 43°29'31.2"N, 10°19'01.2"E, 6m, coarse shell gravel, dredge, 22-05-2020; 2 spms, paratypes and  
783 paragenophores, DBUA0002409.04-05, 43°29'31.2"N, 10°19'01.2"E, 6m, coarse shell gravel,  
784 dredge, 22-05-2020. Collected by Joachim Langeneck.

785

786 *Other material.* Italy, Ischia: 1 spm, DBUA0002408.01, 40°44'42.0"N, 13°56'20.4"E, 6m,  
787 coarse shell gravel, dredge, 10/05/2010; Italy, Antignano: 1 spm, DBUA0002409.01,  
788 43°27'57.6"N, 10°20'24.0"E, 4m, coarse shell gravel, dredge, 05/05/2010; 1 spm,  
789 DBUA0002409.03, 43°29'31.2"N, 10°19'01.2"E, 6m, coarse shell gravel, dredge, 22-05-2020..  
790 Collected by Joachim Langeneck. All specimens, including the holotype and paratypes, are  
791 preserved in ethanol 96% and deposited at the Biological Research Collection (Marine  
792 Invertebrates) of the Department of Biology of the University of Aveiro (COBI at DBUA), Portugal.

792

793 *Diagnosis*

794 Member of *Essc* with type G pigmentation (Table 4), i.e., with white pigmentation dorsally  
795 on prostomium and white transverse dorsal dots across segments (Fig. 6C). Live specimens  
796 present yellow colouration. Antennae slightly longer than palps. Dorsal cirri on segment 2 twice

797 as long as cirri on segment 1, with similar ratio as *E. fenwicki* sp. nov., *E. schanderi* sp. nov, *E*  
798 *gretathunbergae* sp. nov and *E. elektra*, but smaller than *E. pleijeli* sp. nov. (almost three times  
799 as long). Dorsal cirri of median segments large, 1.45 times longer rather than wider, sharing a  
800 similar ratio as *E. fenwicki* sp. nov., *E. pleijeli* sp. nov., *E. gretathunbergae* sp. nov and *E. elektra*,  
801 but smaller than *E. schanderi* sp. nov (twice as long). Ventral cirri of median segments almost  
802 twice as long rather than wider, sharing a similar ratio as *E. fenwicki* sp. nov., *E. schanderi* sp.  
803 nov., *E. gretathunbergae* sp. nov and *E. elektra*, but greater than *E. pleijeli* sp. nov (1.5 times as  
804 long). Proboscis not observed. Worms small, usually between 7 to 11 mm long, with 70 segments.

805

#### 806 *Molecular data*

807 COI, 16S, ITS, and 28S sequences as in specimens DBUA0002408.01;  
808 DBUA0002409.01-05 (Table S1). Phylogenetic relationship as in Fig. 2A, B, with high support  
809 values and low intraspecific (<3%) genetic divergence for both mitochondrial and nuclear  
810 markers. Mean interspecific COI distances to the nearest and farthest neighbours are 15.4%  
811 (K2P, *E. maia*) and 22.0 (K2P, *E. mackiei*), respectively. DOI for the species' Barcode Index  
812 Number (BIN): [dx.doi.org/10.5883/BOLD:AEH2035](https://dx.doi.org/10.5883/BOLD:AEH2035)

813

#### 814 *Etymology*

815 The new species is named after Joachim Langeneck for his sampling efforts and kindness  
816 in providing unique Mediterranean *Eumida* specimens on the behalf of the authors of this paper.

817

#### 818 *Distribution and habitat*

819 Western Mediterranean Sea – Italy, 3 – 6 m depth, on coarse shell gravel.

820

#### 821 *Remarks*

822 Morphologically similar to *E. sanguinea sensu stricto* (Örsted, 1843), except for  
823 pigmentation pattern. Type G pigmentation is unique among the *Essc* and can solely be used to  
824 identify this species. Type G and E pigmentation, are the only pigmentation types with white  
825 pigmentation dorsally on the prostomium up to the middle of the eyes. The latter being exclusive  
826 to *E. notata* found only in Madeira Island (Portugal).

827

## 828 DISCUSSION

829

### 830 NEW SPECIES AND UNNAMED LINEAGES

831 All members of the *Essc*, including the five new species, displayed COI genetic distances  
832 comparable to those found among established species of polychaetes (e.g., Carr *et al.*, 2011;  
833 Lobo *et al.*, 2016; Sampieri *et al.*, 2021). However, the results of nuclear markers in *E. schanderi*  
834 sp. nov. are unexpected due to their customary low divergence with COI. Vieira *et al.* (2019) also  
835 found a similar occurrence when comparing COI and 18S rRNA for one of the MOTUs of  
836 *Dynamene magnitorata* Holdich, 1968 (Isopoda), reporting evidence of cryptic lineages between

837 the Iberian Peninsula and Macaronesia islands. This could be a case of heterozygosity at nuclear  
838 loci (Sota & Vogler, 2003); however, overlapping spikes were not found when analysing the trace  
839 files for *E. schanderi* sp. nov. Besides, the distance between these haplotypes was perhaps too  
840 large to be attributed to heterozygotic variation. Another more plausible scenario is that  
841 hybridization and introgression of mtDNA from a non-sampled lineage could explain the presence  
842 of the same COI haplotype in two different sister lineages (Bachtrog *et al.*, 2006).

843 Although our molecular data support species hypothesis for most new lineages, there are  
844 a few exceptions in the nuclear MOTUs 23, 24, 25, and 27. Each of them is composed of at least  
845 two corresponding distinct mitochondrial lineages. At first, these patterns can either be explained  
846 by hybridization or differential substitution rates among loci. It is because some loci would display  
847 more consolidated lineage sorting stages than others. However, except for *E. merope* and *E. aff.*  
848 *merope* (MOTU 24), no nuclear haplotypes are shared. Therefore, although broader sampling  
849 and balanced representation of sequences from different loci are needed, hybridization could be  
850 discarded. MOTU 24 also did not share haplotypes between *E. notata* and either *E. merope* or *E.*  
851 *aff. merope*. However, regardless of the species status, it is evident these lineages have diverged  
852 recently. When considering only the COI genetic distances (for which there is extensive data),  
853 they appear to be on the lower boundary of customary congeneric distances reported either within  
854 consolidated *Eumida* species (Teixeira *et al.*, 2020) or even compared to polychaetes in general  
855 (Nygren *et al.*, 2009; Ravara *et al.*, 2017). Indeed, *E. aff. merope* displays a mean COI genetic  
856 distance of 10 and 8% to *E. merope* and *E. notata*, respectively, with limited morphometric  
857 differences (Fig. 9) as well. Similar values can be found between *E. kelaino* (MOTU 18) and *E.*  
858 *aff. kelaino* (MOTU 17) or between *E. grethathunbergae* sp. nov. (MOTU 12) and *E. aff.*  
859 *gretathunbergae* (MOTU 13), with 12 and 13% mean COI divergence, respectively, and each pair  
860 sharing the same nuclear MOTU. A comparative analysis by Teixeira *et al.* (2020) indicated that  
861 *Essc* species with COI divergence below 10% may have little or no differentiation in ITS or 28S.  
862 In our study, the same was observed for 16S since the mean distances range between those two  
863 nuclear markers (Table 2). Some exceptions to this pattern can be found in *E. pleijeli* sp. nov.  
864 (MOTU 3) and *Eumida* ORB997 (MOTU 2). In these, a mean COI divergence of 18% was  
865 observed associated with different pigmentation types, but only 1.5% in the ITS region. Alternative  
866 divergence patterns between nuclear and mitochondrial markers have been reported for other  
867 cryptic species as well (e.g., *Notophylum* Örsted, 1843). In this regard, although low mean COI  
868 K2P distances were found between shallow and deep water populations (8.5%), mean distances  
869 for ITS1 (4.9%) were still higher compared to some *Eumida* species analysed here (Nygren *et al.*,  
870 2010).

871 Morphometric data also failed to separate MOTUs with comparatively low genetic  
872 distances between them (<14% COI, Fig. 9). Rice *et al.* (2008) compared genetic distances and  
873 reproductive compatibility in *Polydora cornuta* Bosc, 1802 populations. They reported that signs  
874 of partial larval development can be found between populations with 8% mean COI distances, but  
875 not between those with COI divergence above 15%. Some exceptional cases have also been  
876 reported in marine invertebrates, namely in copepods (Handschumacher *et al.*, 2010). This study

877 showed that, despite the genetic COI distances of above 23% between the Pacific population of  
878 *Tigriopus californicus* (Baker, 1912) and Icelandic *Tigriopus brevicornis* (Müller O.F., 1776), their  
879 crossing can produce mature F1 and F2 hybrids. This, in turn, challenges the restrictive biological  
880 species concept.

881

## 882 PHYLOGEOGRAPHIC INSIGHTS

883 Most *Essc* species have extreme COI haplotype diversity (Table 2). This is comparable  
884 to *Terebellides* Sars, 1835 in Nygren *et al.* (2018), wherein almost all specimens sampled and  
885 sequenced had a unique haplotype in some species. Therefore, additional larvae may have been  
886 recruited from other populations (Meibner *et al.*, 2014). Other polychaete species, such as *Hediste*  
887 Malmgren, 1867, have also shown more than 80 haplotypes in 100 sequences recorded in  
888 species “A” and “B” for both *H. diversicolor* (O.F. Müller, 1776) and *H. atoka* Sato & Nakashima,  
889 2003 (Tosuji *et al.*, 2019). Such high haplotype diversity within species could also be related to  
890 the Pleistocene glaciation (initiated circa 2.8 MY, Maggs *et al.* 2008). Isolated northern ice-free  
891 areas may have allowed pockets of diversity to persist (Stewart & Lister, 2001; Rowe *et al.*, 2004;  
892 Provan & Bennett, 2008). These glacial refuges are areas where some plants or animals survived  
893 during this unfavourable period, with organisms of the same kind extinguished nearby or retracted  
894 southwards to more favourable locations (Andersen & Borns, 1994). It has been proposed that  
895 the Western English Channel is one of the possible locations of coastal glacial refuges (Maggs *et*  
896 *al.*, 2008), thereby close to the Plymouth and Cornwall area, which is home to eight different *Essc*  
897 species, including two of the new species (MOTUs 6 and 12, Fig. 2A, B). Isolation into refugia  
898 reduces geographical ranges and population sizes, resulting in high genetic diversity and high  
899 dissimilarity between refugee populations (Comes & Kadereit, 1998; Willis *et al.*, 2004).

900 The high genetic distance between MOTUs within the *Essc* of the northeast Atlantic  
901 suggests that their diversification likely pre-dates the Pleistocene glaciations. This potential  
902 survival of divergent lineages in common refugia may explain the high level of sympatry currently  
903 observed in this region (Highsmith, 1985; Desiderato *et al.*, 2019).

904

## 905 PIGMENTATION DATA, THE *ESSC* AND MORPHOLOGICAL STASIS

906 Recent studies have suggested that cryptic complexes may remain morphologically  
907 identical due to long periods of morphological stasis (Struck *et al.*, 2018). For example, rates of  
908 morphological evolution in the *Stygocapitella* complex are significantly slower than in closely  
909 related non-cryptic taxa from Nerillidae Levinsen, 1883 and Orbiniidae Hartman, 1942 (Cerca *et*  
910 *al.*, 2020b). Besides the geographic distribution, colouration, and pigmentation, all the new  
911 *Eumida* species examined in this study fail to display any stable and diagnostic morphological  
912 differences, even though slight morphometric variations on the size and shape of the cirri and  
913 prostomial appendages can be found at least between 4 lineages (Table 5). Notably, the outgroup  
914 *E. bahusiensis*, which normally occurs paraphyletically within the *Essc* (Fig. 2), possesses the  
915 same white pigmentation pattern (type B) and the distinct greenish band as does *E. mackiei*  
916 (Teixeira *et al.*, 2020). However, the dorsal cirrus has a visible and larger width that can be

917 identified through traditional morphological approaches (Nygren *et al.*, 2017). Such  
918 micromorphological variations within cryptic and pseudo-cryptic species are seldom detected. For  
919 instance, most *Stygocapitella* lineages lack diagnostic characters and morphological differences  
920 that could allow an unambiguous identification to the species level, including morphometric data  
921 (Cerca *et al.*, 2020a). In a previous study (Teixeira *et al.*, 2020), *E. sanguinea* s. s. also failed to  
922 produce a separated morphometric PCA cluster against three other species from the complex.  
923 Even though in this particular case it could be attributed to bias towards juveniles among the  
924 examined specimens, the likelihood of finding overlapping morphometric variation is still high  
925 when dealing with more than fifteen different *Eumida* species. This PCA result and, in particular,  
926 our new morphometric data for *E. aff. merope* (Fig. 9) could also be indicative of phenotypic  
927 plasticity (e.g., in the proportions of several morphological structures). This phenomenon is  
928 widespread across invertebrates since different phenotypes occur associated with particular  
929 environmental conditions (Fusco & Minelli, 2010; Forsman, 2015), but still scarcely studied in  
930 polychaetes (Nygren & Pleijel, 2011; Syomin *et al.*, 2017). Environmental features could be an  
931 explanation for this variation. In the *Syllis gracilis* Grube, 1840 complex (Langeneck *et al.*, 2020),  
932 a univariate analysis of morphological characters showed that marine specimens sampled on  
933 intertidal algal communities are differentiated from brackish-water and *Sabellaria*-associated  
934 individuals.

935 Pronounced phenotype changes without molecular divergence are also patent in the  
936 *Essc*. Aside from the lack of apparent correlation between geographic occurrence and species  
937 with colour polymorphism (such as *E. merope*, *E. aff. merope*, *E. schanderi* sp. nov., *E.*  
938 *gretathunbergae* sp. nov., and *E. aff. gretathunbergae*), *E. elektra* and *E. taygete* populations had  
939 all their sequences grouped in the same respective MOTU, but geographically different  
940 populations had distinct pigmentations. The latter had an exceptionally wide geographical range  
941 within the *Essc*, from Great Britain to the western and eastern Mediterranean. Yet, the individuals  
942 from the British population possess a distinct pigmentation type (Table 4) and several unique  
943 haplotypes (Fig. 3). Interestingly, reports have often attributed the deep divergence in  
944 invertebrates between eastern and western Mediterranean to the Messinian salinity crisis around  
945 6 MY (e.g., Hupalo *et al.*, 2019; Rögl, 1999). The same is not observed in *E. taygete*, suggesting  
946 recent colonization of the Mediterranean. In this case, neither the morphotype nor geographic  
947 location alone could be indicative of a new species within the *Eumida* complex unless  
948 complemented with molecular data. Such a contrast, for example between *Eumida pleijeli* sp.  
949 nov. and *Eumida langenecki* sp. nov., a combination among collection location, live colouration,  
950 and white pigmentation type is sufficient to successfully identify these species within the *Essc*.

951

## 952 CONCLUSIONS

953 The combination of morphometric and genetic data successfully validated the existence  
954 of three new undescribed species within the *Essc*, namely *E. schanderi* sp. nov., *E. fenwicki* sp.  
955 nov., and *E. gretathunbergae* sp. nov. Since morphometric scatter plots seem to be informative  
956 only for at least five specimens with optimal conditions, such methodology cannot be used for the



957 remaining eight newly detected MOTUs. However, combining colour, white pigmentation types,  
958 and geographic distribution was enough to successfully identify two additional new species, *E.*  
959 *pleijeli* sp. nov. and *E. langenecki* sp. nov., rising to fifteen the total number of species described  
960 within this complex. Our results also suggest that morphometric data alone may not provide  
961 enough resolution for the most genetically close *Eumida* species (i.e., with about less than 14%  
962 COI divergence) and/or cases where nuclear data fail to split into the same number of MOTUs as  
963 mtDNA. Moreover, the probability of finding overlapping morphometric variation for any of the  
964 analysed proportions is high when dealing with more than fifteen different *Eumida* species.  
965 Although genetically similar, the sister species *E. notata* and *E. merope* had at least two different  
966 morphometric markers, did not share haplotypes, and also differed in pigmentation type and  
967 geographic distribution, strengthening their status as independent species. Ideally, studies  
968 examining reproductive compatibility between populations could help clarify the species status of  
969 the lineages referred to as *E. aff. merope*, *E. aff. kelaino*, and *E. aff. gretathunbergae* compared  
970 to their respective sister species. The remaining three new undescribed *Eumida* lineages in this  
971 work (RO174-180, ANT002 and ORB997) will join *Eumida* F22 from Nygren & Pleijel (2011) as  
972 putative species within the *Essc*, with further sampling efforts still needed to clarify their status.

973 The underlying mechanisms behind morphological stasis are still unknown and remain  
974 controversial in evolutionary biology (Fišer *et al.*, 2018). In this sense, combining molecular  
975 phylogenetic tools and examination of small morphological changes can help understand stasis  
976 in species complexes. This can eventually allow for more formal and widespread recognition of  
977 cryptic and pseudo-cryptic biodiversity in biomonitoring and ecological studies.

978

#### 979 CONFLICT OF INTERESTS

980 The authors declare no conflicts of interest

981

#### 982 REFERENCES

983

984 **Andersen BG, Borns HW. 1994.** The ice age world. An introduction to Quaternary history and  
985 research with emphasis on North American and Northern Europe during the last 2.5 million  
986 years. Oslo: Scandinavian University Press, 208.

987 **Bachtrog D, Thornton K, Clark A, Andolfatto P. 2006.** Extensive Introgression of Mitochondrial  
988 Dna Relative to Nuclear Genes in the *Drosophila* Yakuba Species Group. *Evolution* 60: 292–  
989 302.

990 **Barfuss MHJ. 2012.** Molecular studies in Bromeliaceae: Implications of plastid and nuclear DNA  
991 markers for phylogeny, biogeography, and character evolution with emphasis on a new  
992 classification of Tillandsioideae. Vienna: University of Vienna, 244. Available from:  
993 <http://othes.univie.ac.at/24037>

994 **Bely AE, Wray GA. 2004.** Molecular phylogeny of nauidid worms (Annelida: Clitellata) based on  
995 cytochrome oxidase I. *Molecular Phylogenetic and Evolution* 30: 50–63.

- 996 **Bianchi CN, Morri C, Chiantore M, Montefalcone M, Parravicini V, Rovere A. 2012.**  
997 Mediterranean Sea biodiversity between the legacy from the past and a future of change. In:  
998 Stambler N, ed. *Life in the Mediterranean Sea: A Look at Habitat Changes*. New York: Nova  
999 Science Publishers, 1–55.
- 1000 **Bouckaert R, Heled J, Kühnert D, Vaughan T, Wu CH, Xie D, Suchard MA, Rambaut A,**  
1001 **Drummond AJ. 2014.** BEAST 2: A Software Platform for Bayesian Evolutionary Analysis.  
1002 *PLOS Computational Biology* 10: e1003537.
- 1003 **Carr CM, Hardy SM, Brown TM, Macdonald TA, Hebert PDN. 2011.** A Tri-Oceanic Perspective:  
1004 DNA Barcoding Reveals Geographic Structure and Cryptic Diversity in Canadian Polychaetes.  
1005 *PLOS ONE* 6: e22232.
- 1006 **Castresana J. 2000.** Selection of Conserved Blocks from Multiple Alignments for Their Use in  
1007 Phylogenetic Analysis. *Molecular Biology and Evolution* 17: 540–552.
- 1008 **Cazaux C. 1970.** Recherches sur l'écologie et le développement larvaires des Polychètes de la  
1009 région d'Archachon. Thesis, Université de Bordeaux.
- 1010 **Cerca J, Meyer C, Purschke G, Struck TH. 2020a.** Delimitation of cryptic species drastically  
1011 reduces the geographical ranges of marine interstitial ghost-worms (Stygocapitella; Annelida,  
1012 Sedentaria). *Molecular Phylogenetics and Evolution* 143: 106663.
- 1013 **Cerca J, Meyer C, Stateczny D, Siemon D, Wegbrod J, Purschke G, Dimitrov D, Struck TH.**  
1014 **2020b.** Deceleration of morphological evolution in a cryptic species complex and its link to  
1015 paleontological stasis. *Evolution* 74: 116–131.
- 1016 **Churchill CKC, Valdés Á, Foighil DÓ, Churchill CKC, Valdés Á, Foighil DÓ. 2014.** Molecular  
1017 and morphological systematics of neustonic nudibranchs (Mollusca : Gastropoda : Glaucidae :  
1018 Glaucus), with descriptions of three new cryptic species. *Invertebrate Systematics* 28: 174–  
1019 195.
- 1020 **Clement M, Snell Q, Walke P, Posada D, Crandall K. 2002.** TCS: estimating gene genealogies.  
1021 *Proceedings 16th International Parallel and Distributed Processing Symposium*. Ft.  
1022 Lauderdale, FL: IEEE, 7 pp.
- 1023 **Comes HP, Kadereit JW. 1998.** The effect of Quaternary climatic changes on plant distribution  
1024 and evolution. *Trends in Plant Science* 3: 432–438.
- 1025 **Costa FO, Carvalho GR. 2010.** New insights into molecular evolution: prospects from the  
1026 Barcode of Life Initiative (BOLI). *Theory in Biosciences* 129: 149–157.
- 1027 **Crossman CA, Taylor EB, Barrett-Lennard LG. 2016.** Hybridization in the Cetacea: widespread  
1028 occurrence and associated morphological, behavioral, and ecological factors. *Ecology and*  
1029 *Evolution* 6: 1293–1303.
- 1030 **Darriba D, Taboada GL, Doallo R, Posada D. 2012.** jModelTest 2: more models, new heuristics  
1031 and parallel computing. *Nature Methods* 9: 772–772.

- 1032 **Day JH. 1967.** A monograph on the Polychaeta of Southern Africa. London: British Museum  
1033 Natural History. Available at: <http://www.biodiversitylibrary.org/bibliography/8596>
- 1034 **Delić T, Trontelj P, Rendoš M, Fišer C. 2017.** The importance of naming cryptic species and  
1035 the conservation of endemic subterranean amphipods. *Scientific Reports* 7: 3391.
- 1036 **Desiderato A, Costa FO, Serejo CS, Abbiati M, Queiroga H, Vieira PE. 2019.** Macaronesian  
1037 islands as promoters of diversification in amphipods: The remarkable case of the family  
1038 Hyalidae (Crustacea, Amphipoda). *Zoologica Scripta* 48: 359–375.
- 1039 **Eibye-Jacobsen D. 1991.** A revision of *Eumida* Malmgren, 1865 (Polychaeta: Phyllodocidae).  
1040 *Steenstrupia* 17: 81–140.
- 1041 **Fišer C, Robinson CT, Malard F. 2018.** Cryptic species as a window into the paradigm shift of  
1042 the species concept. *Molecular Ecology* 27: 613–635.
- 1043 **Folmer O, Black M, Hoeh W, Lutz R, Vrijenhoek R. 1994.** DNA primers for amplification of  
1044 mitochondrial cytochrome c oxidase subunit I from metazoan invertebrates. *Molecular Marine*  
1045 *Biology and Biotechnology* 3: 294–299.
- 1046 **Forsman A. 2015.** Rethinking phenotypic plasticity and its consequences for individuals,  
1047 populations and species. *Heredity* 115: 276–284.
- 1048 **Fraïsse C, Belkhir K, Welch JJ, Bierne N. 2016.** Local interspecies introgression is the main  
1049 cause of extreme levels of intraspecific differentiation in mussels. *Molecular Ecology* 25: 269–  
1050 286.
- 1051 **Fujisawa T, Barraclough TG. 2013.** Delimiting Species Using Single-Locus Data and the  
1052 Generalized Mixed Yule Coalescent Approach: A Revised Method and Evaluation on  
1053 Simulated Data Sets. *Systematic Biology* 62: 707–724.
- 1054 **Fusco G, Minelli A. 2010.** Phenotypic plasticity in development and evolution: facts and  
1055 concepts. *Philosophical Transactions of the Royal Society B: Biological Sciences* 365: 547–  
1056 556.
- 1057 **Futuyma DJ. 2010.** Evolutionary Constraint and Ecological Consequences. *Evolution* 64: 1865–  
1058 1884.
- 1059 **Glasby CJ, Read GB, Lee KE, Blakemore RJ, Fraser PM, Pinder AM, Erséus C, Moser WE,**  
1060 **Burreson EM, Govedich FR, Davies RW, Dawson EW. 2009.** Phylum Annelida:  
1061 bristleworms, earthworms, leeches. In: Gordon DP, ed. *New Zealand inventory of biodiversity:*  
1062 *volume 1. Kingdom Animalia: Radiata, Lophotrochozoa, Deuterostomia.* Canterbury:  
1063 Canterbury University Press, 312-358.
- 1064 **Guindon S, Gascuel O. 2003.** A Simple, Fast, and Accurate Algorithm to Estimate Large  
1065 Phylogenies by Maximum Likelihood. *Systematic Biology* 52: 696–704.

- 1066 **Handschumacher L, Steinarsdóttir MB, Edmands S, Ingólfsson A. 2010.** Phylogeography of  
1067 the rock-pool copepod *Tigriopus brevicornis* (Harpacticoida) in the northern North Atlantic, and  
1068 its relationship to other species of the genus. *Marine Biology* 157: 1357–1366.
- 1069 **Hassouna N, Mithot B, Bachellerie J-P. 1984.** The complete nucleotide sequence of mouse  
1070 28S rRNA gene. Implications for the process of size increase of the large subunit rRNA in  
1071 higher eukaryotes. *Nucleic Acids Research* 12: 3563–3583.
- 1072 **Highsmith R. 1985.** Floating and algal rafting as potential dispersal mechanisms in brooding  
1073 invertebrates. *Marine Ecology Progress Series* 25: 169–179.
- 1074 **Hupało K, Teixeira MAL, Rewicz T, Sezgin M, Iannilli V, Karaman GS, Grabowski M, Costa  
1075 FO. 2019.** Persistence of phylogeographic footprints helps to understand cryptic diversity  
1076 detected in two marine amphipods widespread in the Mediterranean basin. *Molecular  
1077 Phylogenetics and Evolution* 132: 53–66.
- 1078 **Jumars PA, Dorgan KM, Lindsay SM. 2015.** Diet of Worms Emended: An Update of Polychaete  
1079 Feeding Guilds. *Annual Review of Marine Science* 7: 497–520.
- 1080 **Katoh K, Standley DM. 2013.** MAFFT Multiple Sequence Alignment Software Version 7:  
1081 Improvements in Performance and Usability. *Molecular Biology and Evolution* 30: 772–780.
- 1082 **Kessing B, Croom H, Martin A McIntosh C, McMillan WO, Palumbi S. 1989.** The Simple Fool's  
1083 Guide to PCR (Version 1.0). University of Hawaii, Honolulu.
- 1084 **Kumar S, Stecher G, Li M, Knyaz C, Tamura K. 2018.** MEGA X: Molecular Evolutionary  
1085 Genetics Analysis across Computing Platforms. *Molecular Biology and Evolution* 35: 1547–  
1086 1549.
- 1087 **Langeneck J, Scarpa F, Maltagliati F, Sanna D, Barbieri M, Cossu P, Mikac B, Galletti MC,  
1088 Castelli A, Casu M. 2020.** A complex species complex: The controversial role of ecology and  
1089 biogeography in the evolutionary history of *Syllis gracilis* Grube, 1840 (Annelida, Syllidae).  
1090 *Journal of Zoological Systematics and Evolutionary Research* 58: 66–78.
- 1091 **Leigh JW, Bryant D. 2015.** popart: full-feature software for haplotype network construction.  
1092 *Methods in Ecology and Evolution* 6: 1110–1116.
- 1093 **Leite BR, Vieira PE, Troncoso JS, Costa FO. 2019.** Combining artificial substrates, morphology  
1094 and DNA metabarcoding for investigating macrozoobenthic communities in NW Iberia.  
1095 *Frontiers in Marine Science*. Conference Abstract: XX Iberian Symposium on Marine Biology  
1096 Studies (SIEBM XX) . doi: 10.3389/conf.fmars.2019.08.00061
- 1097 **Librado P, Rozas J. 2009.** DnaSP v5: a software for comprehensive analysis of DNA  
1098 polymorphism data. *Bioinformatics* 25: 1451–1452.
- 1099 **Lobo J, Teixeira MAL, Borges LMS, Ferreira MSG, Hollatz C, Gomes PT, Sousa R, Ravara  
1100 A, Costa MH, Costa FO. 2016.** Starting a DNA barcode reference library for shallow water

- 1101 polychaetes from the southern European Atlantic coast. *Molecular Ecology Resources* 16:  
1102 298–313.
- 1103 **Maggs CA, Castilho R, Foltz D, Henzler C, Jolly MT, Kelly J, Olsen J, Perez KE, Stam W,**  
1104 **Väinölä R, Viard F, Wares J. 2008.** Evaluating Signatures of Glacial Refugia for North Atlantic  
1105 Benthic Marine Taxa. *Ecology* 89: S108–S122.
- 1106 **Martin D, Meca MA, Gil J, Drake P, Nygren A. 2017.** Another brick in the wall: population  
1107 dynamics of a symbiotic species of *Oxydromus* (Annelida, Hesionidae), described as new  
1108 based on morphometry. *Contributions to Zoology* 86: 181–211.
- 1109 **Meibner K, Bick A, Guggolz T, Götting M. 2014.** Spionidae (Polychaeta: Canalipalpata:  
1110 Spionida) from seamounts in the NE Atlantic. *Zootaxa* 3786: 201–245.
- 1111 **Nygren A, Eklöf J, Pleijel F. 2009.** Arctic-boreal sibling species of *Paranaitis* (Polychaeta,  
1112 Phyllodocidae). *Marine Biology Research* 5: 315–327.
- 1113 **Nygren A, Eklöf J, Pleijel F. 2010.** Cryptic species of *Notophyllum* (Polychaeta: Phyllodocidae)  
1114 in Scandinavian waters. *Organisms Diversity & Evolution* 10: 193–204.
- 1115 **Nygren A, Parapar J, Pons J, Meißner K, Bakken T, Kongsrud JA, Oug E, Gaeva D, Sikorski**  
1116 **A, Johansen RA, Hutchings PA, Lavesque N, Capa M. 2018.** A mega-cryptic species  
1117 complex hidden among one of the most common annelids in the North East Atlantic. *PLOS*  
1118 *ONE* 13: e0198356.
- 1119 **Nygren A, Pleijel F. 2011.** From one to ten in a single stroke – resolving the European *Eumida*  
1120 *sanguinea* (Phyllodocidae, Annelida) species complex. *Molecular Phylogenetics and Evolution*  
1121 58: 132–141.
- 1122 **Nygren A, Samuelsson H, Pleijel F. 2017.** The Encyclopedia of the Swedish Flora and Fauna,  
1123 Ringmaskar: Havsborstmaskar. Annelida: Polychaeta: Aciculata. Uppsala: ArtDatabanken.
- 1124 **Pleijel F. 1993.** Polychaeta. Phyllodocidae. *Marine Invertebrates of Scandinavia* 8: 1–159
- 1125 **Provan J, Bennett KD. 2008.** Phylogeographic insights into cryptic glacial refugia. *Trends in*  
1126 *Ecology & Evolution* 23: 564–571.
- 1127 **Puillandre N, Lambert A, Brouillet S, Achaz G. 2012.** ABGD, Automatic Barcode Gap  
1128 Discovery for primary species delimitation. *Molecular Ecology* 21: 1864–1877.
- 1129 **Rambaut A, Drummond AJ, Xie D, Baele G, Suchard MA. 2018.** Posterior Summarization in  
1130 Bayesian Phylogenetics Using Tracer 1.7. *Systematic Biology* 67: 901–904.
- 1131 **Ratnasingham S, Hebert PDN. 2013.** A DNA-Based Registry for All Animal Species: The  
1132 Barcode Index Number (BIN) System. *PLOS ONE* 8: e66213.
- 1133 **Ravara A, Cunha MR, Pleijel F. 2010.** Nephtyidae (Annelida, Polychaeta) from southern Europe.  
1134 *Zootaxa* 2682: 1–68.

- 1135 **Ravara A, Ramos D, Teixeira MAL, Costa FO, Cunha MR. 2017.** Taxonomy, distribution and  
1136 ecology of the order Phyllodocida (Annelida, Polychaeta) in deep-sea habitats around the  
1137 Iberian margin. *Deep Sea Research Part II: Topical Studies in Oceanography* 137: 207–231.
- 1138 **Rice SA, Karl S, Rice KA. 2008.** The *Polydora cornuta* complex (Annelida: Polychaeta) contains  
1139 populations that are reproductively isolated and genetically distinct. *Invertebrate Biology* 127:  
1140 45–64.
- 1141 **Rögl F. 1999.** Mediterranean and Parathetys. Facts and hypothesis of an oligocene to Miocene  
1142 paleogeography (Short Overview). *Geologica Carpathica* 50: 339-349.
- 1143 **Ronquist F, Huelsenbeck JP. 2003.** MrBayes 3: Bayesian phylogenetic inference under mixed  
1144 models. *Bioinformatics* 19: 1572–1574.
- 1145 **Rouse GW. 2006.** Annelid Larval Morphology. *Reproductive Biology and Phylogeny of Annelida:*  
1146 151–188.
- 1147 **Rowe KC, Heske EJ, Brown PW, Paige KN. 2004.** Surviving the ice: Northern refugia and  
1148 postglacial colonization. *Proceedings of the National Academy of Sciences* 101: 10355–  
1149 10359.
- 1150 **Sampieri BR, Steiner TM, Baroni PC, Silva CF da, Teixeira MAL, Vieira PE, Costa FO,**  
1151 **Amaral ACZ. 2020.** How oogenesis analysis combined with DNA barcode can help to  
1152 elucidate taxonomic ambiguities: a polychaete study-based approach. *Biota Neotropica* 20.
- 1153 **Sampieri BR, Vieira P, Teixeira MA, Seixas VC, Pagliosa P, Amaral A, Costa F. 2021.**  
1154 Molecular diversity within the genus *Laeonereis* (Annelida, Nereididae) along the west Atlantic  
1155 coast: paving the way for integrative taxonomy. *PeerJ* 9:e11364
- 1156 **Sota T, Vogler AP. 2003.** Reconstructing species phylogeny of the carabid beetles *Ohomopterus*  
1157 using multiple nuclear DNA sequences: heterogeneous information content and the  
1158 performance of simultaneous analyses. *Molecular Phylogenetics and Evolution* 26: 139–154.
- 1159 **Stewart JR, Lister AM. 2001.** Cryptic northern refugia and the origins of the modern biota. *Trends*  
1160 *in Ecology & Evolution* 16: 608–613.
- 1161 **Struck TH, Feder JL, Bendiksbj M, Birkeland S, Cerca J, Gusarov VI, Kistenich S, Larsson**  
1162 **KH, Liow LH, Nowak MD, Stedje B, Bachmann L, Dimitrov D. 2018.** Finding Evolutionary  
1163 Processes Hidden in Cryptic Species. *Trends in Ecology & Evolution* 33: 153–163.
- 1164 **Syomin V, Sikorski A, Bastrop R, Köhler N, Stradomsky B, Fomina E, Matishov D. 2017.**  
1165 The invasion of the genus *Marenzelleria* (Polychaeta: Spionidae) into the Don River mouth  
1166 and the Taganrog Bay: morphological and genetic study. *Journal of the Marine Biological*  
1167 *Association of the United Kingdom* 97: 975–984.

1168 **Teixeira MAL, Vieira PE, Pleijel F, Sampieri BR, Ravara A, Costa FO, Nygren A. 2020.**  
1169 Molecular and morphometric analyses identify new lineages within a large *Eumida* (Annelida)  
1170 species complex. *Zoologica Scripta* 49: 222–235.

1171 **Thompson JD, Higgins DG, Gibson TJ. 1994.** CLUSTAL W: improving the sensitivity of  
1172 progressive multiple sequence alignment through sequence weighting, position-specific gap  
1173 penalties and weight matrix choice. *Nucleic Acids Research* 22: 4673–4680.

1174 **Tosuji H, Bastrop R, Götting M, Park T, Hong JS, Sato M. 2019.** Worldwide molecular  
1175 phylogeny of common estuarine polychaetes of the genus *Hediste* (Annelida: Nereididae), with  
1176 special reference to interspecific common haplotypes found in southern Japan. *Marine*  
1177 *Biodiversity* 49: 1385–1402.

1178 **Vieira PE, Desiderato A, Holdich DM, Soares P, Creer S, Carvalho GR, Costa FO, Queiroga**  
1179 **H. 2019.** Deep segregation in the open ocean: Macaronesia as an evolutionary hotspot for low  
1180 dispersal marine invertebrates. *Molecular Ecology* 28: 1784–1800.

1181 **Walker AJM, Rees EIS. 1980.** Benthic ecology of Dublin Bay in relation to sludge dumping:  
1182 Fauna.

1183 **Willis KJ, Bennett KD, Walker D, Hewitt GM. 2004.** Genetic consequences of climatic  
1184 oscillations in the Quaternary. *Philosophical Transactions of the Royal Society of London.*  
1185 *Series B: Biological Sciences* 359: 183–195.

1186 **WoRMS Editorial Board (2021).** World Register of Marine Species. Available from  
1187 <http://www.marinespecies.org> at VLIZ. Accessed 2021-05-24. doi:10.14284/170

1188 **Zhang J, Kapli P, Pavlidis P, Stamatakis A. 2013.** A general species delimitation method with  
1189 applications to phylogenetic placements. *Bioinformatics* 29: 2869–2876.

1190  
1191  
1192  
1193  
1194

Marker	Primer	Fragment	Direction (5'- 3')	PCR thermal cycling conditions	Reference
COI	PolyLCO	658bp	(F) GAYTATWTTCAACAAATCATAAAGATATTGG	1) 94 °C (1 min); 2) 5 cycles: 94 °C (40 s), 45 °C (40 s), 72 °C (1 min); 3) 35 cycles: 94 °C (40 s), 51 °C (40 s), 72 °C (1 min); 4) 72 °C (5 min).	Carr <i>et al.</i> (2011)
	PolyHCO		(R) TMACTTCWGGGTGACCAAARAATCA		
COI	LCO1490	658bp	(F) GGTCAACAAATCATAAAGATATTGG	1) 94 °C (1 min); 2) 5 cycles: 94 °C (30 s), 45 °C (1 min 30 s), 72 °C (1 min); 3) 35 cycles: 94 °C (30 s), 51 °C (1 min 30 s), 72 °C (1 min); 4) 72 °C (5 min).	Folmer <i>et al.</i> (1994)
	HCO2198		(R) TAAACTTCAGGGTGACCAAAAAATCA		
	COI-E		(R) TATACTTCTGGGTGTCCGAAGAATCA		
16S	16SAR-L	c.368bp	(F) CGCCTGTTTATCAAAAACAT	1) 94 °C (3 min); 2) 40 cycles: 94 °C (30 s), 47 °C (30 s), 72 °C (1 min); 3) 72 °C (7 min).	Bely <i>et al.</i> (2004) Kessing <i>et al.</i> 1989
	16SANN-F		(F) GCGGTATCCTGACCGTRCWAAGGTA		
	16SBR-H		(R) CCGGTCTGAACTCAGATCACGT		
ITS1	ITS18Sfa	c.675bp	(F) GAGGAAGTAAAAGTCGTAACA		Barfuss (2012)
	ITS5.8Sra		(R) GTTCAATGTGTCCTGCAATTC		
ITS2	ITS5.8SF	c.375bp	(F) ATGCTTAAATTCAGCGGGT	1) 96 °C (4 min); 2) 45 cycles: 94 °C (30 s), 48 °C (30 s), 72 °C (1 min); 3) 72 °C (8 min).	Nygren <i>et al.</i> (2009)
	28SR		(R) GAATTGCAGGACACATTGAAC		
28S	28sC1	c.791bp	(F) ACCCGCTGAATTTAAGCAT		Hassouna <i>et al.</i> (1984)
	28s-D2		(R) TCCGTGTTTCAAGACGG		

1195

1196 **Table 1.** Primers and PCR conditions used in this study.

1197

1198

1199

1200

1201

1202



	Marker	MOTUs	Minimum Distance (%)	Mean Distance (%)	Maximum distance (%)
Within MOTUs	COI		0	0.59	3.8
	16S	All	0	0.18	0.8
	ITS		0	0.44	5.8*
	28S		0	0.06	0.8*
Between MOTUs	COI		5.5	16.7	23.4
	16S	All	0.3	7.6	15.1
	ITS		0.5	9.2	18.1
	28S		0	1.7	4.5
Most similar MOTUS	COI	9 vs 11	7.6	8.2	8.7
		9 vs 10	5.5	6.7	7.4
		10 vs 11	9.8	10.2	10.6
	16S	10 vs 11	0.3	0.3	0.5
		9 vs 11	0.4	0.4	0.5
		9 vs 10	0.5	0.7	0.8
	ITS	17 vs 18	0.5	0.5	0.9
		2 vs 3	1.5	1.5	1.5
		12 vs 13	1.4	1.9	3.4
		10 vs 11	0	0	0
28S	20 vs 16	0.1	0.1	0.1	
	17 vs 18	0.3	0.3	0.4	
Most distant MOTUs	COI	1 vs 13	20.5	21.7	23.4
		1 vs 5	21.1	22	22.6
		2 vs 12	21.1	21.8	22.9
	16S	2 vs 15	15.1	15.1	15.1
		2 vs 22	14.1	14.4	14.4
		1 vs 15	13.7	13.8	14.1
	ITS	1 vs 14	17.4	17.6	18.1
		3 vs 14	15	15.1	15.2
		2 vs 14	15.4	15.5	15.6
	28S	2 vs 12	3.7	3.8	4.5
2 vs 13		3.5	3.6	3.7	
5 vs 13		3.4	3.5	3.6	

1203

1204 **Table 2.** Mean intra and interspecific genetic distances (K2P) among all the *Essc* for the four  
1205 analysed markers (COI, 16S, ITS and 28S), with focus on the distances between MOTUs in  
1206 relation to the three closest and distant neighbours

1207

1208

1209

1210

1211

1212

1213

1214

1215









1216

1217

1218

	Region	N	h	Hd	S	Pi	Fu and Li's D	Tajima's D
<i>E. schanderi</i> sp. nov.	BSW, BNO	13	6	0.72	4	0,0015	-1,60955 P > 0.10	-1,43759 P > 0.10
<i>E. fenwicki</i> sp. nov.	ANO, CGB, PGB, RFR	23	10	0,73	11	0,0022	-1,33065 P > 0.10	<b>-1,87001</b> <b>P &lt; 0.05</b>
<i>E. gretathunbergae</i> sp. nov.	PGB	26	24	0.99	39	0.0089	-2.10801 0.10 > P > 0.05	-1.77253 0.10 > P > 0.05
<i>Eumida</i> RO174-180	RFR	2	2	1.0	1	0,0016	-	-
<i>E. aff. gretathunbergae</i>	RFR, PGB	2	2	1.0	3	0,0048	-	-
<i>E. aff. kelaino</i>	BFR	2	1	0.0	-	-	-	-
<i>Eumida</i> ANT002	AIT	1	1	-	-	-	-	-
<i>E. pleijeli</i> sp. nov.	NIT	2	1	0.0	-	-	-	-
<i>E. langenecki</i> sp. nov.	AIT	5	5	1.0	11	0,0073	-0,92693 P > 0.10	-0,92693 P > 0.10
<i>Eumida</i> ORB997	OIT	1	1	-	-	-	-	-
<i>E. aff. merope</i>	RFR, PGB	13	8	0,86	11	0,0033	-1,94450 0.10 > P > 0.05	-1,70303 0.10 > P > 0.05
<i>E. merope</i>	BFR, ICR	10	8	0.93	32	0,0060	0,19975 P > 0.10	0,84167 P > 0.10
<i>E. notata</i>	FPT	11	10	0,98	24	0,0092	-1,27851 P > 0.10	-1,47163 P > 0.10
<i>E. mackiei</i>	PGB	28	26	0,99	37	0,0081	<b>-2,69971</b> <b>P &lt; 0.05</b>	-1,71525 0.10 > P > 0.05
<i>E. sanguinea</i>	BSW, FNO, BNO, PGB, SGB, HDEN	31	14	0,82	26	0,0073	-0,06960 P > 0.10	-1,06336 P > 0.10
<i>E. maia</i>	PGB, CGB, BFR	39	24	0,91	42	0,0084	<b>-2,61094</b> <b>P &lt; 0.05</b>	-1,71386 0.10 > P > 0.05
<i>E. alkyone</i>	BNO, DNO, BSW	8	7	0,96	16	0,0082	-1,09777 P > 0.10	-0,85599 P > 0.10
<i>E. elektra</i>	BNO, RFR	15	4	0,70	5	0,0030	0,48090 P > 0.10	0,76339 P > 0.10
<i>E. taygete</i>	BFR, CGB, PGB, IIT	22	18	0,98	35	0,0111	-0,49631 P > 0.10	-1,07113 P > 0.10
<i>E. kelaino</i>	BSW, PGB, SNO, BNO, RFR	21	10	0,81	10	0,0038	-1,00506 P > 0.10	-0,50678 P > 0.10
<i>E. asterope</i>	BFR	2	2	1.0	1	0,0016	-	-
<i>Eumida</i> F22	BFR	1	1	-	-	-	-	-

1220 **Table 3.** Indices of genetic diversity estimated, based on COI for each MOTU. Number of  
1221 sequences (n); nucleotide diversity ( $\pi$ ), number of haplotypes (h), haplotype diversity (Hd) and  
1222 number of variables sites (S). Region abbreviations as stated in the methods, with the addition of:  
1223 DENH, Denmark, Helsingør; CRI, Croatia, Istra; GBS, Great Britain, Scilly Islands and PTM,  
1224 Portugal, Madeira island.

Combination Type	On Prostomium	Dorsally on Segment 2 <sup>a</sup>	Dorsal Transverse Lines <sup>b</sup>	Dorsal Longitudinal Line	Dorsal Transverse Dots	Dorsal Eye-like Pattern	Species
A 	-	X	X	-	-	-	<i>E. alkyone</i> ; <i>E. maia</i> ; <b><i>E. merope</i></b> ; <b><i>E. aff. merope</i></b> , <i>E. mackiei</i> ; <i>E. asterope</i> ; <b><i>E. elektra</i></b> ; <b><i>E. taygete</i></b> ; <b><i>E. gretathunbergae</i> sp. nov.</b> ; <b><i>E. schanderi</i> sp. nov.</b> ; <i>E. fenwicki</i> sp. nov.; <i>Eumida</i> RO174-180; <b><i>E. aff. gretathunbergae</i></b>
B 	-	-	-	-	-	-	<i>E. kelaino</i> ; <i>E. aff. kelaino</i> ; <i>Eumida pleijeli</i> sp. nov.
C 	-	X	-	X	-	-	<i>E. sanguinea</i> ; <b><i>E. merope</i></b> ; <b><i>E. aff. merope</i></b> , <b><i>E. taygete</i></b> , <i>Eumida</i> F22; <b><i>E. schanderi</i> sp. nov.</b> ; <i>Eumida</i> ANT002; <b><i>E. elektra</i></b>
D 	-	X	-	-	-	-	<i>E. notata</i>
E 	X	-	-	-	-	-	<b><i>E. gretathunbergae</i> sp. nov.</b> ; <b><i>E. aff. gretathunbergae</i></b>
F 	-	-	X	-	-	-	<i>E. langenecki</i> sp. nov.
G 	X	-	-	-	X	-	<i>Eumida</i> ORB997
H 	-	X	-	-	-	X	

1225 <sup>a</sup> Specimens with pigmentation dorsally on segment 2 may also have various amounts of pigmentation on the anterior cirri and in the prostomium.

1226 <sup>b</sup> Transverse lines in some specimens from *Eumida merope*, *Eumida cf merope* and *E. aff. gretathunbergae* are very short, approaching spots.

1227

1228 **Table 4.** Patterns of white pigmentation in the *Eumida sanguinea* species complex with eight unique combinations (types A–H). Species in bold have polymorphic  
1229 pigmentation types.

	<i>E. fenwicki</i> sp. nov.	<i>E. schanderi</i> sp. nov.	<i>E.</i> <i>gretathunbergae</i> sp. nov.	<i>E. elektra</i>	<i>E. pleijeli</i> sp. nov.	<i>E. langenecki</i> sp. nov.
AL/PL	2 ( <b>AL &gt; PL</b> )	1 ( <b>AL &lt; PL</b> )	3 ( <b>AL &lt; PL</b> )	4 (AL > PL)	AL > PL	AL > PL
AL/HL	<b>2</b>	<b>1</b>	3 (larger head)	4	-	-
AL/HW	<b>2</b>	<b>1</b>	3 (larger head)	4	-	-
AL/MAL	2	<b>1</b>	2	3	-	-
AL/STL	<b>2</b>	<b>1</b>	3 (larger tentacles)	4	-	-
AL/LTL	<b>2</b>	<b>1</b>	3 (larger tentacles)	4	-	-
NS (mean)	56	45	<b>94</b>	61	70	59
DCL>DCW	1,5x	<b>1.9x</b>	1.5x	1.5x	1.5x	1.45x
VCL>VCW	2x	2x	2x	2x	1.5x	2x
DCS2L>CS1L	2x	2x	2x	2x	<b>2.7x</b>	2x
WL (mean, mm)	5	4	<b>14</b>	7	9	12
Pigmentation	B	B and D	B and <b>F</b>	B	<b>C</b>	<b>G</b>
Live Coloration	Light Yellow	<b>Greenish</b>	Yellowish-brown	Yellowish	<b>Green</b>	Yellow
Distribution	NE Atlantic	<b>Scandinavia</b>	<b>Great Britain</b>	NE Atlantic	<b>Green</b> <b>Western</b> <b>Mediterranean</b> <b>Sea</b>	<b>Western</b> <b>Mediterranean</b> <b>Sea</b>

1230

1231 **Table 5.** Summary of the most relevant morphometric findings rating from 1 (smaller proportions) to 4 (larger proportions), number of segments (NS), ratio  
1232 between the length and width of the dorsal cirri of median segments (DCL>DCW), ventral cirri of media segments (VCL>VCW) and the length between the  
1233 dorsal cirri on segment 2 against the cirri on segment 1 (DCS2>CS1L), worm length (WL), pigmentation type, live coloration and geographical range regarding  
1234 the new described species and *E. elektra*. Data in bold has the most distinct differences when combined

1235

1236

1237

1238

1239

1240

1241 **Table and figure captions**

1242

1243 **Table 1.** Primers and PCR conditions used in this study.

1244

1245 **Table 2.** Mean intra and interspecific genetic distances (K2P) among all the *Essc* for the four  
1246 analysed markers (COI, 16S, ITS and 28S), with focus on the distances between MOTUs in  
1247 relation to the three closest and distant neighbours.

1248

1249 **Table 3.** Indices of genetic diversity estimated, based on COI for each MOTU. Number of  
1250 sequences (n); nucleotide diversity ( $\pi$ ), number of haplotypes (h), haplotype diversity (Hd) and  
1251 number of variable sites (S). Region abbreviations as stated in the methods, with the addition of:  
1252 DENH, Denmark, Helsingør; CRI, Croatia, Istra; GBS, Great Britain, Scilly Islands and PTM,  
1253 Portugal, Madeira island.

1254

1255 **Table 4.** Patterns of white pigmentation in the *Eumida sanguinea* species complex with eight  
1256 unique combinations (types A–H). Species in bold have polymorphic pigmentation types.

1257

1258 **Table 5.** Summary of the most relevant morphometric findings rating from 1 (smaller proportions)  
1259 to 4 (larger proportions), number of segments (NS), ratio between the length and width of the  
1260 dorsal cirri of median segments (DCL>DCW), ventral cirri of media segments (VCL>VCW) and  
1261 the length between the dorsal cirri on segment 2 against the cirri on segment 1 (DCS2>CS1L),  
1262 worm length (WL), pigmentation type, live coloration and geographical range regarding the new  
1263 described species and *E. elektra*. Data in bold has the most distinct differences when combined  
1264

1265

1266 **Fig.1.** Schematic of the *E. sanguinea* morphotype (modified from Teixeira *et al.* (2020)) showing  
1267 the measurements used in the morphometric analysis (A, B). A, Anterior end. B, Parapodia.  
1268 Abbreviations: CLL, the length of the chaetigerous lobes; CLH, the height of the chaetigerous  
1269 lobes; AL, the length of the antennae; PL, the length of the palps; MAL, the length of the middle  
1270 antenna; CS1L, cirri on segment 1; DCS2L, dorsal cirri on segment 2; DCL, the length of the  
1271 dorsal cirri; VCL, the length of the ventral cirri; HL, the length of the head; WWP, the width of the  
1272 worm with parapodia; WW, the width of the worm without parapodia; HW, the width of the head;  
1273 DCW, the width of the dorsal cirri; VCW, the width of the ventral cirri; DE, distance between the  
1274 eyes.

1274

1275 **Fig.2.** Phylogenetic tree reconstructed using Bayesian inference for the *Essc* (A, B), comparing  
1276 296 COI and 94 16S concatenated mitochondrial sequences (A) against 192 combined nuclear  
1277 markers from the ITS-region and 28S sequences (B), with information regarding the different  
1278 MOTU delineation methods. BINs were used only for COI. Collapsed clades have less than 3.5%  
1279 genetic divergence. Numbers in parenthesis indicate the number of sequences used for each  
1280 MOTU and in the case of the mitochondrial markers the first correspond to COI and the second

1281 to 16S. *Eumida ockelmanni*, *Eumida aff. ockelmanni*, *Sige fusigera* and *Eumida bahusiensis* as  
1282 outgroups. Only the bootstrap values over 0.85 BI support are shown. Each different consensus  
1283 MOTU is represented by the respective number, with the colored ones corresponding to the  
1284 described species and new lineages found in this study. Abbreviations: Cons MOTU, Consensus  
1285 MOTU; OUTG, Outgroup.

1286

1287 **Fig.3.** Haplotypes networks based on COI for all the *Essc* and respective outgroups. Each  
1288 haplotype is represented by a circle and number of haplotypes are according to the displayed  
1289 scale. Colours indicate the geographic location of the haplotype. Numbers correspond to the  
1290 number of mutational steps between haplotypes. Lines without numbers means only one mutation  
1291 between haplotypes.

1292

1293 **Fig.4.** Haplotypes networks based on ITS (A), 28S (B) and 16S (C) for all the *Essc* and respective  
1294 outgroups. Each haplotype is represented by a circle and number of haplotypes are according to  
1295 the displayed scale. Colours indicate the geographic location of the haplotype. Numbers  
1296 correspond to the number of mutational steps between haplotypes. Lines without numbers means  
1297 only one mutation between haplotypes.

1298

1299 **Fig.5.** Live, relaxed *Eumida* specimens exhibiting different types of white pigmentation patterns  
1300 and coloration (A-F). A, *Eumida schanderi* sp. nov., specimen ZMBN\_134559 (size: 3.3 mm), with  
1301 green coloration and type B pigmentation and (B) specimen ZMBN\_134556 (size: 3.7 mm,  
1302 holotype) with type D pigmentation and focus on the prostomium. C, *Eumida gretathunbergae* sp.  
1303 nov., specimen DBUA0002400.01 (size: 15 mm, holotype) exhibiting type F pigmentation, and  
1304 (D) specimen DBUA0002400.03 (size: 13 mm) exhibiting type B pigmentation. E, *Eumida fenwicki*  
1305 sp. nov., specimen DBUA0002396.01 (size 5 mm, holotype) exhibiting type B pigmentation. F,  
1306 *Eumida* RO174-180, specimen DBUA0002403.01 (size: 10 mm) exhibiting type B pigmentation.  
1307 Darker yellow color results from the stomach content.

1308

1309 **Fig.6.** Live, relaxed *Eumida* specimens exhibiting different types of white pigmentation patterns  
1310 and coloration (A-E). A, *Eumida aff. merope*, specimen DBUA0002393.01 exhibiting type A  
1311 pigmentation and (B) specimen DBUA0002395.02 displaying type D pigmentation. C, *Eumida*  
1312 *langenecki* sp. nov., specimen DBUA0002408.01, with type G pigmentation. D, *Eumida pleijeli*  
1313 sp. nov., specimen DBUA0002407.02, displaying its characteristic green coloration mixed with  
1314 type C pigmentation. E, *Eumida* ORB997, specimen DBUA0002410.01, with type H pigmentation.  
1315 All the specimens are similar in size measuring around 12 mm, except for DBUA0002410.01  
1316 measuring around 6.3 mm.

1317

1318 **Fig.7.** Live, relaxed *Eumida* specimens exhibiting the different types of white pigmentation  
1319 patterns and coloration (A-C). A, *Eumida aff. kelaino.*, specimen DBUA0002404.01 exhibiting type  
1320 C pigmentation. B, *Eumida aff. gretathunbergae*, specimen DBUA0002401.01 displaying type F

1321 pigmentation with very small transverse lines. C, *Eumida* ANT002, specimen DBUA0002405.01  
1322 exhibiting type D pigmentation. All the specimens are similar in size measuring around 14 mm,  
1323 except for DBUA0002405.01 measuring around 3 mm.

1324

1325 **Fig.8.** Scatter plots with the most significant proportions in distinguishing *E. fenwicki* sp. nov.,  
1326 *E. schanderi* sp. nov., *E. gretathungergae* sp. nov and *E. elektra* from each other (A-H).  
1327 Morphometric proportions between the length of the antennae - AL and (A) short tentacular length  
1328 - STL; (B) large tentacular length - LTL; (C) head width - HW; (D) head length - HL; (E) palp length  
1329 - PL and (F) the length of the middle antenna - MAL. Measurements between the number of  
1330 segments - NS against (G) the worm width – WW and (H) worm length - WL.

1331

1332 **Fig.9.** Scatter plots with the most significant proportions in distinguishing *E. notata*, *E. merope*,  
1333 *E. aff. merope* and *E. elektra* from each other (A-F). Morphometric measurements between (A)  
1334 worm width - WW and worm width with parapodia - WWP; (B) antennae length - AL and palp  
1335 length - PL; (C) head length - HL with antennae length - AL; (D) distance between the eyes – DE  
1336 and head width - HW; (E) ventral cirri length - VCL with dorsal cirri length - DCL and (F)  
1337 chaetigerous lobe length – CLL against the ventral cirri length - VCL.

1338

1339

#### 1340 SUPPORTING INFORMATION

1341

1342 Additional Supporting Information can be found in the online version of this article at the  
1343 publisher's web-site:

1344

1345 **Table S1.** Voucher data from Nygren *et al.* (2016), Teixeira *et al.* (2020) and this study. Origin of  
1346 the specimens used in the molecular work, pigmentation types, vouchers and GenBank accession  
1347 numbers for each of the analysed genetic markers. Separate accession numbers were assigned  
1348 for ITS1 and ITS2 regarding data from Teixeira *et al.* (2020), while the records from Nygren and  
1349 Pleijel (2011) and this study have a single accession number for the entire ITS region.

1350

1351 **Table S2.** Morphometric measurements for all the specimens belonging to the new species *E.*  
1352 *schanderi* sp. nov., *E. fenwicki* sp. nov., *E. gretathunbergae* sp. nov., *E. pleijeli* sp. nov., *E.*  
1353 *langenecki* sp. nov., as well for *E. notata*, *E. merope*, *E. aff. merope* and *E. elektra*.

1354

1355 **Fig. S1.** Maximum likelihood phylogenies for the concatenated mitochondrial (COI and 16S)  
1356 dataset

1357

1358 **Fig. S2.** Maximum likelihood phylogenies for the concatenated nuclear (ITS and 28S) dataset

1359

1360